A Generic Small-Signal Stability Criterion of DC Distribution Power System: Bus Node Impedance Criterion (BNIC)

Bangbang He, *Student Member, IEEE*, Wu Chen, *Senior Member, IEEE*, Xinbo Ruan, *Fellow, IEEE*, Xin Zhang, *Senior Member, IEEE*, Zhixiang Zou, *Senior Member, IEEE*, and Wu Cao, *Member, IEEE*

***Abstract*—The dc distribution power system has drawn widespread attention and rapidly developed in recent years; however, its stability issue is one of the urgent challenges, requiring much attention. In previous stability studies, the line impedance network is often overlooked, which is convenient for the geographically centralized systems, but inaccurate for the distributed systems. In this article, the modeling and stability criteria of these two systems are simultaneously studied. For the distributed systems, first, the transfer functions from each input voltage or current disturbance to the bus voltage are derived. On this basis, the sufficient and necessary condition for the system stability is discussed. Subsequently, a bus node impedance criterion (BNIC) is proposed to assess the small-signal stability of the dc distribution power system. For the centralized systems, by ignoring the line impedance network, its small-signal model can be deduced by the distributed system, and the proposed BNIC is proved to be still valid. In addition, some existing impedance-based stability criteria are analyzed and compared with the proposed BNIC. Finally, the correctness and effectiveness of the proposed BNIC are verified by the cases study and experiments.**

***Index Terms*—Bus node impedance criterion (BNIC), dc distribution power system, line impedance network, Nyquist criterion, small-signal stability.**

Nomenclature

BCCC	Bus-current-controlled converter.
BNIC	Bus node impedance criterion.
BVCC	Bus-voltage-controlled converter.
CCM	Component connection method.
CPL	Constant power load.
ESR	Equivalent series resistance.
FFT	Fast Fourier transform.
PBSC	Passivity-based stability criterion.
RHP	Right-half-plane.

Manuscript received May 26, 2021; revised August 3, 2021, September 28, 2021, and November 4, 2021; accepted November 27, 2021. Date of publication December 1, 2021; date of current version January 19, 2022. This work was supported in part by the National Natural Science Foundation of China under Award 51922028, in part by the National Key Research and Development Program of China under Grant 2018YFB0904100, and in part by the Science and Technology Project of State Grid under Grant SGHB0000KXJS1800685. Recommended for publication by Associate Editor M. Molinas. *(Corresponding author: Wu Chen.)*

Bangbang He, Wu Chen, Zhixiang Zou, and Wu Cao are with the Center for Advanced Power Conversion Technology and Equipment, School of Electrical Engineering, Southeast University, Nanjing 210096, China (e-mail: he_bangbang@163.com; chenwu@seu.edu.cn; zzou@seu.edu.cn; caowu_ee@seu.edu.cn).

Xinbo Ruan is with the Center for More-Electric-Aircraft Power Systems, College of Automation Engineering, Nanjing University of Aeronautics and Astronautics, Nanjing 211106, China (e-mail: ruanxb@nuaa.edu.cn).

Xin Zhang is with the College of Electrical Engineering, Zhejiang University, Hangzhou 310027, China (e-mail: zhangxin_ieee@zju.edu.cn).

Color versions of one or more figures in this article are available at https://doi.org/10.1109/TPEL.2021.3131700.

Digital Object Identifier 10.1109/TPEL.2021.3131700

I. Introduction

With the high penetration of photovoltaic, wind power and energy storage systems [1]–[3], as well as the increase of dc loads [4], the dc distribution power system has been widely studied and developed. Nevertheless, due to the complex interaction between subsystems and the negative impedance characteristic of constant power load (CPL), the stability issue is still a big challenge [5]–[13], which is closely concerned by academia and industry.

The stability issues of the dc distribution power system can be divided into small-signal and large-signal stability issues [14]–[16]. The small-signal stability is mainly studied for the stability of bus voltage around the system equilibrium point, which needs to linearize the system [17], [18]. While the large-signal stability analysis adopts nonlinear mathematical methods to evaluate the self-balancing ability of bus voltage under a large disturbance (such as pulse load, load steps, start up, and fault events) [15], [19]. This article only focuses on the small-signal stability of the dc distribution power system.

At present, the impedance-based analysis method and the eigenvalue analysis method are mainly adopted to evaluate the small-signal stability of power-electronic systems [20]–[22]. For the eigenvalue analysis method, the state-space model of the whole system needs to be established; hence, researchers must fully understand the detailed parameter information, internal structure, and configuration [23], [24], which is contradictory to the protection of user privacy and trade secrets [25]. Moreover, with the increase of system scale, the matrix order of the state-space model increases sharply, which will lead to the additional calculation problems and analysis difficulty [26], [27]. Relatively speaking, considering the impedance characteristics of each subsystem is more advantageous than analyzing its detailed internal characteristics [28], especially for the system regarded as a "black box" [24], [26]. Therefore, the impedance-based analysis method is becoming more and more popular [29]–[31].

Impedance-based analysis method was first proposed by Middlebrook in 1976 and applied to design input filter of a dc system [32]. The Middlebrook criterion points out that when both source and load converters are individually stable, the cascaded system will be stable as long as the source output impedance $Z_{\rm o}$ is always less than the load input impedance $Z_{\rm in}$ in entire frequency range, namely the impedance-ratio $Z_{\rm o}/Z_{\rm in}$ is less than 1. Subsequently, various impedance-based stability criteria have been reported during the past decades.

For example, in order to reduce the conservatism of the Middlebrook criterion and provide the system parameter design standard, a series of impedance criteria based on forbidden region are reported, but these criteria are just the sufficient conditions of system stability [7], [33], [34]. Contrary to the Middlebrook criterion, for the cascaded system with a current-controlled source, its stability depends on the reversed impedance-ratio $Z_{\rm in}/Z_{\rm o}$ [35]. In general, in the dc distribution power system, any converter can be classified as a bus-voltage-controlled converter (BVCC) or a bus-current-controlled converter (BCCC), then, if the impedance-ratio of BVCC and BCCC satisfies the Nyquist criterion, the whole system is stable [36]. For these existing impedance-ratio criteria, it is necessary to know all converter types in order to determine the correct impedance-ratio [37]. However, the impedance-sum criterion reported in [37] and [38] does not require the type of converters to be distinguished, and it can be applicable to any cascaded system consisting of two converters/sources. In addition, Cao *et al.* [39] proposed a global-admittance criterion for the multi-parallel inverter-based power system, that is, the system is stable if the admittance-sum of all converters/subsystems has no right-half-plane (RHP) zeros. Different from the above stability criteria, a passivity-based stability criterion (PBSC) was reported in [40]. If the passivity of the bus impedance is guaranteed, the stability is ensured as well, but the reverse is not necessarily true [33]. Therefore, the PBSC is also the sufficient condition of system stability.

In the aforementioned research articles, due to the neglect of the line impedance network, these criteria may not be directly applied to the geographically distributed system [41]. In order to overcome this problem, the component connection method (CCM) is introduced to study the stability of complex network systems [42]. According to the CCM, all converters or subsystems are expressed as a matrix equation, and the network characteristic is illustrated by the node admittance matrix. Subsequently, some related works and stability criteria are reported [23], [41], [43]–[50]. However, if there is a huge number of sources and loads exist in the power network, the orders of these two matrices will be very high. In this case, although the CCM can reduce the computation burden of deducing and establishing the system transfer function matrices [23], [49], it is still difficult to evaluate the system stability based on a large size transfer function matrix. Therefore, the stability criterion based on the CCM must be further simplified or a simpler one needs to be proposed.

When analyzing the stability of the dc distribution system, the only difference between geographically centralized system and distributed system is whether the line impedance network is considered. In this article, the small-signal models and stability conditions of these two systems are simultaneously studied, and a bus node impedance criterion (BNIC) is proposed. Then, the mathematical derivation, cases study and experimental verification show that, no matter whether line impedance network is considered or not, the proposed BNIC is always generic and valid.

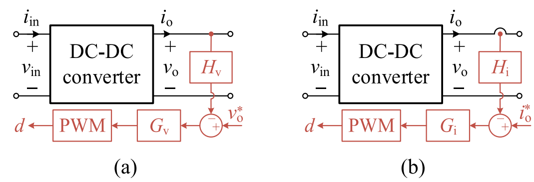

Fig. 1. DC–DC converter and its control block diagram. (a) Output-voltage-control mode. (b) Output-current-control mode.

The rest of this article is organized as follows. In Section II, the two-port small-signal model and simplified model of dc–dc converter are given. In Section III, for the dc distribution power system considering the line impedance network, its small-signal model is established and the BNIC is proposed. In Section IV, the line impedance network of the dc distribution power systems is ignored and its small-signal model is built. On this basis, some exiting stability criteria are analyzed and compared with the proposed BNIC. In Section V, the case study and experimental research are carried out. Finally, Section VI concludes this article.

II. Two-Port Small-Signal Model of DC–DC Converter and Its Simplification

Before adopting the impedance-based stability analysis method, the small-signal model of each dc–dc converter should be determined. The dc–dc converters with the output-voltage-control and the output-current-control modes are illustrated in Fig. 1. Here, $v_{\rm in}$ and $i_{\rm in}$ are the input voltage and current, respectively; $v_{\rm o}$ and $i_{\rm o}$ are the output voltage and current, respectively; $H_{\rm v}$ and $H_{\rm i}$ are the feedback coefficients of the output voltage and current, respectively; $G_{\rm v}$ and $G_{\rm i}$ are the transfer functions of the voltage-loop and current-loop controllers, respectively; d is the duty cycle.

Considering the above two control modes, the two-port small-signal model of the dc–dc converter can be expressed as (1) and (2), respectively [4]. Here, $\hat{v}_{\rm in}$ and $\hat{i}_{\rm o}$ are the input disturbances in output-voltage-control mode, while $\hat{v}_{\rm in}$ and $\hat{v}_{\rm o}$ are the input disturbances in output-current-control mode.

$$\begin{bmatrix} \hat{i}_{\rm in} \\ \hat{v}_{\rm o} \end{bmatrix} = \begin{bmatrix} Y_{\rm in} & G_{\rm ii} \\ G_{\rm vv} & -Z_{\rm o} \end{bmatrix} \begin{bmatrix} \hat{v}_{\rm in} \\ \hat{i}_{\rm o} \end{bmatrix} \tag{1}$$

$$\begin{bmatrix} \hat{i}_{\rm in} \\ \hat{i}_{\rm o} \end{bmatrix} = \begin{bmatrix} Y_{\rm in} & G_{\rm voi} \\ G_{\rm vii} & -Y_{\rm o} \end{bmatrix} \begin{bmatrix} \hat{v}_{\rm in} \\ \hat{v}_{\rm o} \end{bmatrix} \tag{2}$$

where $Y_{\rm in} = 1/Z_{\rm in}$ is the input admittance, $G_{\rm ii}$ is the transfer function from $\hat{i}_{\rm o}$ to $\hat{i}_{\rm in}$, $G_{\rm vv}$ is the transfer function from $\hat{v}_{\rm in}$ to $\hat{v}_{\rm o}$, $Z_{\rm o} = 1/Y_{\rm o}$ is the output impedance, $G_{\rm voi}$ is the transfer function from $\hat{v}_{\rm o}$ to $\hat{i}_{\rm in}$, and $G_{\rm vii}$ is the transfer function from $\hat{v}_{\rm in}$ to $\hat{i}_{\rm o}$.

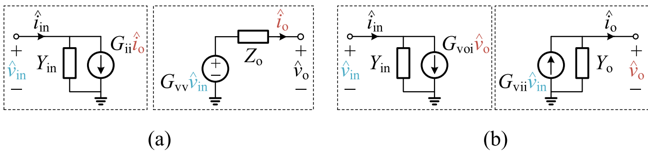

Fig. 2. Two-port small-signal equivalent circuit of the dc–dc converter. (a) Output-voltage-control mode. (b) Output-current-control mode.

According to the classical control theory, when a dc–dc converter operates stably, its four transfer functions of the second-order matrix in (1) or (2) have no RHP poles.

Based on (1) and (2), the two-port small-signal equivalent circuits of dc–dc converters are shown in Fig. 2. Obviously, its left-side and right-side equivalent circuits are decoupled in structure, and each side includes the two input disturbances. Therefore, before establishing the small-signal model of the dc distribution power system, for each dc–dc converter, we can only retain the part of the equivalent circuit connected to the bus side. In this way, all the input disturbances can be remained and the circuit analysis can be simplified significantly.

It should be pointed out that according to the definition of BVCC and BCCC in [36], when a dc–dc converter adopts bus-voltage-control mode, it is classified as a BVCC, while other converters are all considered as the BCCCs. Therefore, combining with the Fig. 2, the Thevenin equivalent model is preferred for the BVCC, while the Norton equivalent model is preferred for the BCCC.

III. Modeling and Stability Criteria of a DC Distribution Power System Considering the Line Impedance Network

A. System Description and Modeling

In the dc distribution power system, if all converters are dispersed geographically, the line impedance network cannot be neglected. In such a situation, the structure of the dc distribution power system is shown in Fig. 3(a). There are r dc–dc converters, including k BVCCs and m BCCCs, and $k + m = r$. The nodes between each converter and bus are denoted by $\mathrm{n}_1, \mathrm{n}_2, \ldots, \mathrm{n}_r$. v_α and i_α $(\alpha = 1, 2, \ldots, r)$ are the voltage and current at the bus node n_α, respectively. In the line impedance network, there is an resistive–inductive line impedance between two connected nodes, and for the longer cables, the capacitance of each node to the ground should also be considered. Note that all these impedances are passive.

The simplified small-signal model of the dc distribution power system are described as Fig. 3(b). Here, for BVCC_k, $Z_{\mathrm{o},k}$ is its output impedance, $v_{\mathrm{c},k}$ is its open-circuit voltage on the bus side, and i_k is its output current; for BCCC_m, $Y_{\mathrm{in},m}$ is its input admittance, $i_{\mathrm{c},m}$ is its short-circuit current on the bus side, and i_{k+m} is its output current. Based on Fig. 2, the input disturbances of each converter are contained in $\hat{v}_{\mathrm{c},k}$ and $\hat{i}_{\mathrm{c},m}$. If BVCC_k and BCCC_m are stable individually, $\hat{v}_{\mathrm{c},k}$ and $\hat{i}_{\mathrm{c},m}$ are bounded, and there are no RHP poles in both $Z_{\mathrm{o},k}$ and $Y_{\mathrm{in},m}$.

In order to facilitate the establishment of the system with the node admittance method, the Thevenin equivalent circuit of each

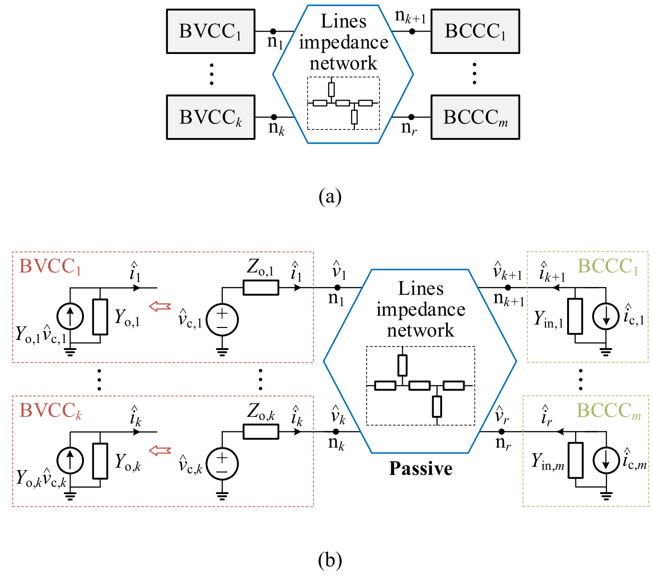

Fig. 3. Structure and model of dc distribution power system. (a) System structure. (b) Simplified small-signal model.

BVCC is replaced by the Norton equivalent circuit, as shown in Fig. 3(b). Here, $Z_{\mathrm{o},k} = 1/Y_{\mathrm{o},k}$. Note that the replacement is reasonable, only for the system modeling and does not affect the subsequent stability analysis. Therefore, the node admittance equation of the system can be expressed as

$$\hat{\boldsymbol{i}} = (\boldsymbol{Y} + \boldsymbol{Y}_{\mathrm{net}})\hat{\boldsymbol{v}} \tag{3}$$

where $\hat{\boldsymbol{i}}$ is the injected current source vector; $\boldsymbol{Y}$ is the admittance matrix of all converters on the bus side; $\boldsymbol{Y}_{\mathrm{net}}$ is the node admittance matrix of the line impedance network, it should be pointed out that if the line parameters are unknown, $\boldsymbol{Y}_{\mathrm{net}}$ can be obtained by measurement, as shown in Appendix-A; $\hat{\boldsymbol{v}}$ is the bus node voltage vector. Notice that the bold variables represent matrices or vectors. The mathematical expressions of $\hat{\boldsymbol{i}}$, $\boldsymbol{Y}$, and $\hat{\boldsymbol{v}}$ are

$$\begin{cases} \hat{\boldsymbol{i}} = (Y_{\mathrm{o},1}\hat{v}_{\mathrm{c},1}, \ldots, Y_{\mathrm{o},k}\hat{v}_{\mathrm{c},k}, -\hat{i}_{\mathrm{c},1}, \ldots, -\hat{i}_{\mathrm{c},m})^{\mathrm{T}} \\ \boldsymbol{Y} = \mathrm{diag}\,(Y_{\mathrm{o},1}, \ldots, Y_{\mathrm{o},k}, Y_{\mathrm{in},1}, \ldots, Y_{\mathrm{in},m}) \\ \hat{\boldsymbol{v}} = (\hat{v}_1, \ldots, \hat{v}_k, \hat{v}_{k+1}, \ldots, \hat{v}_r)^{\mathrm{T}}. \end{cases} \tag{4}$$

Let

$$\begin{cases} \boldsymbol{Z}_{\mathrm{o}} = \mathrm{diag}\,(Z_{\mathrm{o},1}, \ldots, Z_{\mathrm{o},k}, -1, \ldots, -1) \\ \hat{\boldsymbol{h}} = (\hat{v}_{\mathrm{c},1}, \ldots, \hat{v}_{\mathrm{c},k}, \hat{i}_{\mathrm{c},1}, \ldots, \hat{i}_{\mathrm{c},m})^{\mathrm{T}} \\ \boldsymbol{Y}_{\mathrm{in}} = \mathrm{diag}\,(1, \ldots, 1, -Y_{\mathrm{in},1}, \ldots, -Y_{\mathrm{in},m}) \end{cases} \tag{5}$$

where $\hat{\boldsymbol{h}}$ is the disturbance vector.

By comparing (4) and (5), there are

$$\hat{\boldsymbol{i}} = \boldsymbol{Z}_{\mathrm{o}}^{-1}\hat{\boldsymbol{h}} \tag{6}$$

$$\boldsymbol{Y} = \boldsymbol{Z}_{\mathrm{o}}^{-1}\boldsymbol{Y}_{\mathrm{in}}. \tag{7}$$

Substituting (6) and (7) into (3), the relationship between the bus node voltage $\hat{\boldsymbol{v}}$ and the disturbance vector $\hat{\boldsymbol{h}}$ can be further deduced as

$$\hat{\boldsymbol{v}} = (\boldsymbol{Y}_{\mathrm{in}} + \boldsymbol{Z}_{\mathrm{o}}\boldsymbol{Y}_{\mathrm{net}})^{-1}\hat{\boldsymbol{h}}. \tag{8}$$

B. Stability Analysis and Criteria

If all converters operate stably individually, combined with the foregoing analysis and Fig. 2, $\hat{\boldsymbol{h}}$ is bounded. Therefore, the system is stable *if and only if* each transfer function in the matrix $(\boldsymbol{Y}_{\text{in}} + \boldsymbol{Z}_{\text{o}}\boldsymbol{Y}_{\text{net}})^{-1}$ has no RHP poles [44], [49], which is the existing criterion based on the CCM. However, this matrix includes a lot of impedance calculations and each transfer function of it should be evaluated. For this reason, the following *lemma* is proposed to simplify this criterion.

Lemma: Assume that the transfer functions $a_{i,j}$ and $b_{i,j}$ (i, $j = 1, 2, \ldots, \lambda$) have no RHP poles, and λ-order matrices $\boldsymbol{A}$ and $\boldsymbol{B}$ consist of $a_{i,j}$ and $b_{i,j}$, respectively, that is, $\boldsymbol{A} = (a_{i,j})_{\lambda\times\lambda}$, $\boldsymbol{B} = (b_{i,j})_{\lambda\times\lambda}$. Then, 1) the determinant det($\boldsymbol{A}$) has no RHP poles; 2) each transfer function in both the product $\boldsymbol{AB}$ and the adjoint matrix adj($\boldsymbol{A}$) has no RHP poles.

Proof: Based on the calculation formula of the determinant, matrix multiplication and adjoint matrix, there are

$$\det(\boldsymbol{A}) = \sum_{w_1 w_2 \cdots w_\lambda} \left[(-1)^{\tau(w_1 w_2 \cdots w_\lambda)} a_{1,w_1} a_{2,w_2} \cdots a_{\lambda,w_\lambda}\right] \tag{9}$$

$$\boldsymbol{AB} = \left(\sum_{l=1}^{\lambda} a_{i,l} b_{l,j}\right)_{\lambda\times\lambda} \tag{10}$$

$$\text{adj}(\boldsymbol{A}) = (A_{j,i})_{\lambda\times\lambda} \tag{11}$$

where, $w_1 w_2 \ldots w_\lambda$ presents a permutation of $1, 2, \ldots, \lambda$ and $\tau(w_1 w_2 \ldots w_\lambda)$ is its inversion number; $A_{j,i}$ is the algebraic covalent of $a_{i,j}$ and it is a determinant.

Obviously, only the addition and multiplication operations about $a_{i,j}$ and $b_{i,j}$ are included in (9) to (11), and these operations do not introduce RHP poles. Therefore, in the above calculation results, each transfer function does not have RHP poles.

According to the calculation formula of the inverse matrix, the matrix $(\boldsymbol{Y}_{\text{in}} + \boldsymbol{Z}_{\text{o}}\boldsymbol{Y}_{\text{net}})^{-1}$ can be written as

$$(\boldsymbol{Y}_{\text{in}} + \boldsymbol{Z}_{\text{o}}\boldsymbol{Y}_{\text{net}})^{-1} = \frac{\text{adj}(\boldsymbol{Y}_{\text{in}} + \boldsymbol{Z}_{\text{o}}\boldsymbol{Y}_{\text{net}})}{\det(\boldsymbol{Y}_{\text{in}} + \boldsymbol{Z}_{\text{o}}\boldsymbol{Y}_{\text{net}})}. \tag{12}$$

Because all converters are stable individually, each transfer function in $\boldsymbol{Y}_{\text{in}}$ and $\boldsymbol{Z}_{\text{o}}$ has no RHP poles. Meanwhile, for the passive line impedance network, each transfer function in $\boldsymbol{Y}_{\text{net}}$ has no RHP zeros and poles. Based on the above *lemma*, each transfer function in the matrix adj($\boldsymbol{Y}_{\text{in}} + \boldsymbol{Z}_{\text{o}}\boldsymbol{Y}_{\text{net}}$) and determinant det($\boldsymbol{Y}_{\text{in}} + \boldsymbol{Z}_{\text{o}}\boldsymbol{Y}_{\text{net}}$) have no RHP poles. Therefore, the sufficient and necessary condition for the system stability can be simplified as that det($\boldsymbol{Y}_{\text{in}} + \boldsymbol{Z}_{\text{o}}\boldsymbol{Y}_{\text{net}}$) has no RHP zeros or its Nyquist curve does not circle the origin clockwise. Note that the assumption, each converter operates stable individually, is necessary and the precondition of discussing the system stability, because it can ensure the adj($\boldsymbol{Y}_{\text{in}} + \boldsymbol{Z}_{\text{o}}\boldsymbol{Y}_{\text{net}}$) has no RHP poles so that the system stability only depends on the RHP zeros of det($\boldsymbol{Y}_{\text{in}} + \boldsymbol{Z}_{\text{o}}\boldsymbol{Y}_{\text{net}}$).

Obviously, compared with the transfer function matrix $(\boldsymbol{Y}_{\text{in}} + \boldsymbol{Z}_{\text{o}}\boldsymbol{Y}_{\text{net}})^{-1}$, det($\boldsymbol{Y}_{\text{in}} + \boldsymbol{Z}_{\text{o}}\boldsymbol{Y}_{\text{net}}$) is just a determinant-based transfer function and has less impedance calculation, which can be seen from (12), and the more detail derivation is presented in Appendix-B.

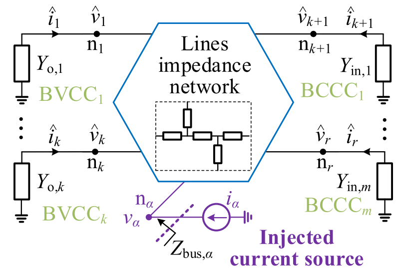

Fig. 4. Equivalent model based on the external power method.

It should be pointed out that the similar stability analysis method for the closed-loop network model has been widely studied, and some determinant-based stability criteria have been proposed in existing publications [51]–[56], such as the nodal admittance matrix-based, loop impedance matrix-based, and return-ratio matrix-based determinant stability criteria. However, almost all of these criteria are based on ac system. In Appendix-C, they are extended to the dc distribution power system based on the proposed det($\boldsymbol{Y}_{\text{in}} + \boldsymbol{Z}_{\text{o}}\boldsymbol{Y}_{\text{net}}$)-based stability criterion. Meanwhile, by comparison, the proposed det($\boldsymbol{Y}_{\text{in}} + \boldsymbol{Z}_{\text{o}}\boldsymbol{Y}_{\text{net}}$)-based stability criterion is proved to be a better choice and has wider application scenarios.

C. Proposed BNIC

Criterion: The dc distribution power system is stable *if and only if* the bus impedance at *any* node has no RHP poles.

Proof: In general, the bus node impedance $Z_{\text{bus},\alpha}$ ($\alpha = 1, 2, \ldots, r$) at the node n_α is considered. As shown in Fig. 4, the external power supply method is used, that is, all current sources in Fig. 3 are set to zero and an external injected current source i_α is connected at node n_α.

In this case, the node admittance equation of the system can be expressed as

$$\hat{i}_\alpha \boldsymbol{\eta}^{\text{T}} = (\boldsymbol{Y} + \boldsymbol{Y}_{\text{net}})\hat{\boldsymbol{v}} \tag{13}$$

where, $\boldsymbol{\eta} = (0, \ldots, 0, \overset{\alpha}{1}, 0, \ldots, 0)_{1\times r}$.

Since there are

$$\hat{i}_\alpha = \boldsymbol{\eta}(\hat{i}_\alpha \boldsymbol{\eta}^{\text{T}}) \tag{14}$$

$$\hat{v}_\alpha = \boldsymbol{\eta}\hat{\boldsymbol{v}}. \tag{15}$$

Substituting (14) and (15) into (13), the bus node impedance $Z_{\text{bus},\alpha}$ can be expressed as

$$\begin{aligned} Z_{\text{bus},\alpha} &= \frac{\hat{v}_\alpha}{\hat{i}_\alpha} = \boldsymbol{\eta}(\boldsymbol{Y} + \boldsymbol{Y}_{\text{net}})^{-1}\boldsymbol{\eta}^{\text{T}} \\ &= \boldsymbol{\eta}\left[(\boldsymbol{Y}_{\text{in}} + \boldsymbol{Z}_{\text{o}}\boldsymbol{Y}_{\text{net}})^{-1}\boldsymbol{Z}_{\text{o}}\right]\boldsymbol{\eta}^{\text{T}} \\ &= \frac{\boldsymbol{\eta}\left[\text{adj}(\boldsymbol{Y}_{\text{in}} + \boldsymbol{Z}_{\text{o}}\boldsymbol{Y}_{\text{net}})\boldsymbol{Z}_{\text{o}}\right]\boldsymbol{\eta}^{\text{T}}}{\det(\boldsymbol{Y}_{\text{in}} + \boldsymbol{Z}_{\text{o}}\boldsymbol{Y}_{\text{net}})}. \end{aligned} \tag{16}$$

Because each transfer function in $\boldsymbol{Y}_{\text{in}}$, $\boldsymbol{Z}_{\text{o}}$, and $\boldsymbol{Y}_{\text{net}}$ has no RHP poles, according to the proposed *lemma*, each transfer function in the matrix adj($\boldsymbol{Y}_{\text{in}} + \boldsymbol{Z}_{\text{o}}\boldsymbol{Y}_{\text{net}}$)$\boldsymbol{Z}_{\text{o}}$ also has no RHP poles. Notice that $\boldsymbol{\eta}[\text{adj}(\boldsymbol{Y}_{\text{in}} + \boldsymbol{Z}_{\text{o}}\boldsymbol{Y}_{\text{net}})\boldsymbol{Z}_{\text{o}}]\boldsymbol{\eta}^{\text{T}}$ presents the element in the α-th row and α-th column of matrix adj($\boldsymbol{Y}_{\text{in}} + \boldsymbol{Z}_{\text{o}}\boldsymbol{Y}_{\text{net}}$)$\boldsymbol{Z}_{\text{o}}$, which means it also has no RHP poles. Therefore,

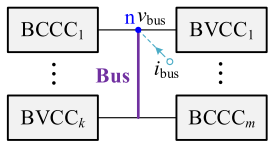

Fig. 5. Structure of the dc distribution power system without considering line impedance network.

whether $Z_{\mathrm{bus},\alpha}$ contains RHP poles is equivalent to whether the determinant det($\boldsymbol{Y}_{\mathrm{in}} + \boldsymbol{Z}_{\mathrm{o}}\boldsymbol{Y}_{\mathrm{net}}$) contains RHP zeros. As aforementioned, the system is stable *if and only if* det($\boldsymbol{Y}_{\mathrm{in}} + \boldsymbol{Z}_{\mathrm{o}}\boldsymbol{Y}_{\mathrm{net}}$) has no RHP zeros. Hence, the stability of the dc distribution power system can be judged by the bus node impedance $Z_{\mathrm{bus},\alpha}$, namely the system is stable *if and only if* $Z_{\mathrm{bus},\alpha}$ has no RHP poles. Since the whole derivation process is independent of the value of α, the system stability can be evaluated by the bus impedance at *any* node. Besides, $Z_{\mathrm{bus},\alpha}$ also has less impedance calculation than the matrix $(\boldsymbol{Y}_{\mathrm{in}} + \boldsymbol{Z}_{\mathrm{o}}\boldsymbol{Y}_{\mathrm{net}})^{-1}$, which will be demonstrated in Appendix-B.

IV. Stability Analysis and Criterion Comparison of the DC Distribution Power System Without Considering Line Impedance Network

A. System Description and Modeling

Most of the existing stability criteria for the dc distribution power system do not consider the line impedance network. In fact, when all converters are concentrated geographically and the transmission lines are short, the structure of the dc distribution power system is shown in Fig. 5. Note that there is only one equivalent node n on the whole bus, and its voltage is denoted by v_{bus}. i_{bus} is the bus current injected by an external equipment.

According to the Fig. 3(b), when the line impedance is ignored, each node voltage is v_{bus}, the cross-line-impedance between any two connected nodes is 0, and the self-line-admittance of each node is 0. Therefore, there are

$$\hat{\boldsymbol{v}} = (\hat{v}_{\mathrm{bus}}, \ldots, \hat{v}_{\mathrm{bus}},\ \hat{v}_{\mathrm{bus}}, \ldots,\ \hat{v}_{\mathrm{bus}})^{\mathrm{T}} = \hat{v}_{\mathrm{bus}}\boldsymbol{\xi}^{\mathrm{T}} \tag{17}$$

$$\boldsymbol{\xi}\boldsymbol{Y}_{\mathrm{net}}\boldsymbol{\xi}^{\mathrm{T}} = 0 \tag{18}$$

where $\boldsymbol{\xi} = (1, 1, \ldots, 1)_{1\times r}$.

Based on (6) and (8), there is

$$(\boldsymbol{Y} + \boldsymbol{Y}_{\mathrm{net}})\hat{\boldsymbol{v}} = \boldsymbol{Z}_{\mathrm{o}}^{-1}\hat{\boldsymbol{h}}. \tag{19}$$

Substituting (17) and (18) into (19), $\hat{v}_{\mathrm{bus}}$ can be expressed as

$$\hat{v}_{\mathrm{bus}} = \frac{\boldsymbol{\xi}\boldsymbol{Z}_{\mathrm{o}}^{-1}}{\boldsymbol{\xi}\boldsymbol{Y}\boldsymbol{\xi}^{\mathrm{T}}}\hat{\boldsymbol{h}} = \frac{\sum_{p=1}^{k} Y_{\mathrm{o},p}\hat{v}_{c,p}}{\sum_{p=1}^{k} Y_{\mathrm{o},p} + \sum_{q=1}^{m} Y_{\mathrm{in},q}} - \frac{\sum_{p=1}^{m} \hat{i}_{c,q}}{\sum_{p=1}^{k} Y_{\mathrm{o},p} + \sum_{q=1}^{m} Y_{\mathrm{in},q}}. \tag{20}$$

B. Stability Analysis and the Proposed BNIC

Based on (20), the sufficient and necessary condition for the system stability is that the transfer function from each disturbance to $\hat{v}_{\mathrm{bus}}$ has no RHP poles. To further analysis, let

$$Z_{\mathrm{o},p} = \frac{1}{Y_{\mathrm{o},p}} = \frac{N_{\mathrm{o},p}}{D_{\mathrm{o},p}},\quad Y_{\mathrm{in},q} = \frac{N_{\mathrm{in},q}}{D_{\mathrm{in},q}} \tag{21}$$

where *N* and *D* are defined as polynomials of *s* (*s* is the Laplace variable), that is, $N_{\mathrm{o},p}$ and $D_{\mathrm{o},p}$ are the numerator and denominator polynomials of $Z_{\mathrm{o},p}$, respectively; $N_{\mathrm{in},q}$ and $D_{\mathrm{in},q}$ are the numerator and denominator polynomials of $Y_{\mathrm{in},q}$, respectively.

It should be pointed out that if all BVCCs and BCCCs are stable individually, $D_{\mathrm{o},p} = 0$ and $D_{\mathrm{in},q} = 0$ have no RHP roots.

Substituting (21) into (20), $\hat{v}_{\mathrm{bus}}$ can be rewritten as (22) shown at the bottom of this page, where, $R_1(s,p)$, $R_2(s)$, and $R(s)$ are all polynomials of *s*.

When all converters are individually stable, $\hat{v}_{\mathrm{c},p}$ and $\hat{i}_{\mathrm{c},q}$ are bounded, therefore, $R(s) = 0$ is the characteristic equation of the dc distribution power system. In other words, the system is stable *if and only if* $R(s) = 0$ has no RHP roots.

As shown in Fig. 5, there is only one equivalent node on the whole bus, therefore, the proposed BNIC can be restated as: the dc distribution power system is stable *if and only if* the bus impedance Z_{bus} has no RHP poles. Here, $Z_{\mathrm{bus}} = \hat{v}_{\mathrm{bus}}/\hat{i}_{\mathrm{bus}}$, which means Z_{bus} is the parallel equivalent impedance of all converters on the bus side. Combining with (21), Z_{bus} can be expressed as

$$Z_{\mathrm{bus}} = Z_{\mathrm{o},1}//\cdots//Z_{\mathrm{o},k}//Z_{\mathrm{in},1}//\cdots//Z_{\mathrm{in},m} = \left(\sum_{p=1}^{k} Y_{\mathrm{o},p} + \sum_{q=1}^{m} Y_{\mathrm{in},q}\right)^{-1} = \frac{1}{R(s)}\prod_{p=1}^{k} N_{\mathrm{o},p}\prod_{q=1}^{m} D_{\mathrm{in},q}. \tag{23}$$

Obviously, the denominator of Z_{bus} is $R(s)$; hence, when Z_{bus} has no RHP poles, the dc distribution power system is stable, which is consistent with the conclusion when considering the line impedance network.

Actually, (23) can also be derived from (16), and the proof process is shown in Appendix-D. In other words, the system

$$\hat{v}_{\mathrm{bus}} = \frac{\prod_{q=1}^{m} D_{\mathrm{in},q}\sum_{p=1}^{k}\left[\left(\prod_{p=1}^{k} N_{\mathrm{o},p}\right)\frac{D_{\mathrm{o},p}}{N_{\mathrm{o},p}}\hat{v}_{c,p}\right] - \prod_{p=1}^{k} N_{\mathrm{o},p}\prod_{q=1}^{m} D_{\mathrm{in},q}\sum_{q=1}^{m}\hat{i}_{c,q}}{\underbrace{\prod_{p=1}^{k} N_{\mathrm{o},p}\prod_{q=1}^{m} D_{\mathrm{in},q}\left(\sum_{p=1}^{k}\frac{D_{\mathrm{o},p}}{N_{\mathrm{o},p}} + \sum_{q=1}^{m}\frac{N_{\mathrm{in},q}}{D_{\mathrm{in},q}}\right)}_{R(s)}} = \frac{\sum_{p=1}^{k} R_1(s,p)\hat{v}_{c,p} - \sum_{q=1}^{m} R_2(s)\hat{i}_{c,q}}{R(s)} \tag{22}$$

shown in Fig. 5 is a special case of Fig. 3 where the line impedance network is neglected, and the proposed BNIC is also applicable.

It should be pointed out that although the concept of the bus impedance has been mentioned in the PBSC [40], [57], and [58], the research ideas, contents, and conclusions of this article are still quite different from them. The comparison with the PBSC will be given in Section IV-C. In [57], the bus impedance was used to estimate the eigenvalues of the cascaded system consisting of two converters, which can be regarded as the eigenvalue analysis method, and the authors declared its application in the large scale, complex, and meshed systems still needs to be investigated in the further work. In [58], the bus impedance of a parallel system is adopted to prove that at the terminal of any of the parallel-connected converters, the impedance-ratio can be used to evaluate the system stability. In other words, the bus impedance is only taken as an intermediate process to prove the proposed impedance-ratio criterion. In addition, the line impedance network did not be considered in the above researches. In our article, the proposed BNIC is the conclusion of strict mathematical deduction and suitable for the more general application scenarios.

C. Comparisons With Some Existing Stability Criteria

At present, for the dc distribution power system shown in Fig. 5, the existing impedance-based stability criteria mainly include: global-admittance criterion, impedance-ratio criterion, impedance-sum criterion, and the PBSC. These criteria will be discussed and compared one by one as follows.

1) Global-Admittance Criterion: The global-admittance is defined as the admittance sum of all converters on the bus side, that is

$$Y_g = \sum_{p=1}^{k} Y_{\mathrm{o},p} + \sum_{q=1}^{m} Y_{\mathrm{in},q} = R(s)\left(\prod_{p=1}^{k} N_{\mathrm{o},p}\prod_{q=1}^{m} D_{\mathrm{in},q}\right)^{-1}. \tag{24}$$

This criterion requires Y_g has no RHP zeros [39]. Obviously, Y_g is the reciprocal of Z_{bus} when the line impedance network is ignored. Hence, this criterion can be used to judge the stability of the system shown in Fig. 5. However, this criterion may not be directly extended to the system shown in Fig. 3 because there are multiple nodes on the bus, which is beyond the definition of the global-admittance.

2) Impedance-Ratio Criterion: The impedance-ratio is defined as the parallel equivalent impedance ratio of all BVCCs and all BCCCs, that is

$$T_{\mathrm{m}} = \frac{Z_{\mathrm{o},1}//\cdots//Z_{\mathrm{o},k}}{Z_{\mathrm{in},1}//\cdots//Z_{\mathrm{in},m}} = \sum_{q=1}^{m} Y_{\mathrm{in},q} \Bigg/ \sum_{p=1}^{k} Y_{\mathrm{o},p}. \tag{25}$$

Combined with (21), there is

$$\frac{1}{1+T_{\mathrm{m}}} = \frac{1}{R(s)}\prod_{q=1}^{m} D_{\mathrm{in},q}\sum_{p=1}^{k}\left[\left(\prod_{p=1}^{k} N_{\mathrm{o},p}\right)\frac{D_{\mathrm{o},p}}{N_{\mathrm{o},p}}\right]. \tag{26}$$

Hence, this criterion requires T_{m} meets the Nyquist criterion [36]. However, the disadvantage of the impedance-ratio criterion is that it is necessary to distinguish the converter type [37], while the proposed BNIC and the global-admittance criterion do not.

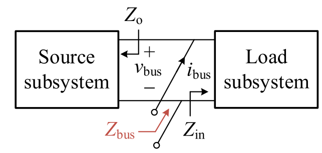

Fig. 6. Definition of bus impedance.

3) Impedance-Sum Criterion: This criterion indicates that two cascaded converters are stable when their impedance-sum has no RHP zeros [37], [38]. For example, if the system shown in Fig. 5 only includes two BVCCs, namely $k = 2$ and $m = 0$, based on (22), there is $R(s) = N_{\mathrm{o},1}D_{\mathrm{o},2} + N_{\mathrm{o},2}D_{\mathrm{o},1}$. The impedance-sum of the two BVCCs can be expressed as (27). Obviously, the molecule of the impedance-sum is $R(s)$.

$$Z_{\mathrm{o},1} + Z_{\mathrm{o},2} = \frac{N_{\mathrm{o},1}}{D_{\mathrm{o},1}} + \frac{N_{\mathrm{o},2}}{D_{\mathrm{o},2}} = \frac{N_{\mathrm{o},1}D_{\mathrm{o},2} + N_{\mathrm{o},2}D_{\mathrm{o},1}}{D_{\mathrm{o},1}D_{\mathrm{o},2}}. \tag{27}$$

Although the impedance-sum criterion is also independent of the converter type, the current research on it mainly focuses on the cascaded system composed of two converters. If Z_{sum} is defined as the sum of the bus-side-impedance of all converters in Fig. 5, it can be seen from (28) that the numerator of Z_{sum} is not $R(s)$. Therefore, this criterion cannot be directly extended to the dc distribution power system. In other words, the application of this criterion in the dc distribution system needs further study [38]

$$\begin{aligned} Z_{\mathrm{sum}} &= Z_{\mathrm{o},1} + \cdots + Z_{\mathrm{o},k} + Z_{\mathrm{in},1} + \cdots + Z_{\mathrm{in},m} \\ &= \prod_{p=1}^{k} D_{\mathrm{o},p}\prod_{q=1}^{m} N_{\mathrm{in},q} \\ &\quad \times \left(\sum_{p=1}^{k}\frac{N_{\mathrm{o},p}}{D_{\mathrm{o},p}} + \prod_{q=1}^{m}\frac{D_{\mathrm{in},q}}{N_{\mathrm{in},q}}\right) \Bigg/ \left(\prod_{p=1}^{k} D_{\mathrm{o},p}\prod_{q=1}^{m} N_{\mathrm{in},q}\right). \end{aligned} \tag{28}$$

4) PBSC: The PBSC is proposed based on the sufficient and necessary condition of the passivity of one-port network, which can be used to analyze the system stability [40], [59]. As illustrated in Fig. 6, this criterion requires the bus impedance $Z_{\mathrm{bus}} = Z_{\mathrm{o}}//Z_{\mathrm{in}}$ meets: 1) Z_{bus} has no RHP poles; 2) $\angle Z_{\mathrm{bus}}(\mathrm{j}\omega) \in [-90^{\circ}, 90^{\circ}]$ or $\mathrm{Re}[Z_{\mathrm{bus}}(\mathrm{j}\omega)] \geq 0$ $(\forall\omega)$.

Different from the PBSC, the proposed BNIC only requires that Z_{bus} has no RHP poles, and does not require that the phase of Z_{bus} falls within the interval $[-90^{\circ}, 90^{\circ}]$ in the whole frequency range. The detailed proof process is as follows.

According to the well-known Cauchy's argument principle [60], if Z_{bus} has no RHP poles, the following conclusions can be obtained.

1) When Z_{bus} has no RHP zeros, the Nyquist curve of Z_{bus} does not encircle the origin.
2) When Z_{bus} has some RHP zeros, the number of times that the Nyquist curve of Z_{bus} encircles the origin clockwise is equal to the number of its RHP zeros.

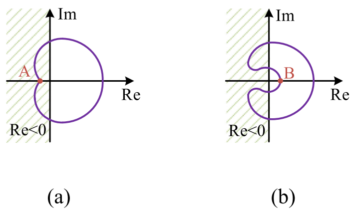

Fig. 7. Typical Nyquist curves. (a) With cross-point A. (b) With cross-point B.

Two typical Nyquist curves are shown in Fig. 7. If the Nyquist curve encircles the origin at least once, there is at least one cross-point A on the negative real axis, otherwise, all cross-points with the real axis are in the RHP [61]. Therefore, when the Nyquist curve of Z_{bus} has cross-points with the negative real axis, its phase frequency characteristic curve will pass through the –180° line at least once, otherwise it will not be. In other words, the system stability is only related to whether the phase frequency characteristic curve of Z_{bus} passes through the -180° line, while the condition $\text{Re}[Z_{\text{bus}}(\text{j}\omega)] \geq 0$ is not required. For example, assume that Z_{bus} has no RHP zeros and its Nyquist curve is shown in Fig. 7(b), the system is stable while a part of the Nyquist curve of Z_{bus} is in the left-half-plane, which means the second condition of the PBSC is not satisfied. Hence the PBSC is just a sufficient condition for system stability. Another example of a stable system but not satisfying $\text{Re}[Z_{\text{bus}}(\text{j}\omega)] \geq 0$ is given in Section V-B.

To sum up, compared with the existing stability criteria, no matter whether line impedance network is considered or not, the proposed BNIC is always a more generic and simple stability criterion for the dc distribution power system.

D. Comparisons of the Two Proposed Criteria

It should be pointed out that, in addition to the BNIC, another stability criterion based on $\det(\boldsymbol{Y}_{\text{in}} + \boldsymbol{Z}_{\text{o}}\boldsymbol{Y}_{\text{net}})$ is also proposed in this article. The comparisons of these two proposed criteria are as follows.

1) The BNIC has a clear physical meaning and is generic for the two types of the dc distribution power systems mentioned in this article, while the $\det(\boldsymbol{Y}_{\text{in}} + \boldsymbol{Z}_{\text{o}}\boldsymbol{Y}_{\text{net}})$-based stability criterion is only applicable to the system considering the line impedance network, the detailed analysis is given in Appendix-E.
2) The proposed BNIC is not perfect, it also suffers a limitation, that is, it requires the detailed transfer functions of all converters, which has the same drawback as the eigenvalue-based stability methods, global-admittance criterion, and impedance-sum criterion. By comparison, the $\det(\boldsymbol{Y}_{\text{in}} + \boldsymbol{Z}_{\text{o}}\boldsymbol{Y}_{\text{net}})$-based stability criterion is better in practical application, because only frequency response is needed in its Nyquist curve, which means the measurement of $\boldsymbol{Y}_{\text{in}}$, $\boldsymbol{Z}_{\text{o}}$, and $\boldsymbol{Y}_{\text{net}}$ are sufficient.

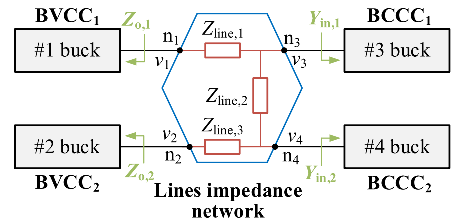

Fig. 8. Structure of a dc distribution power system.

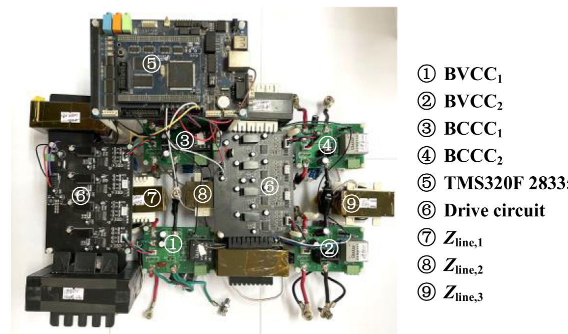

Fig. 9. Schematic diagram of the experimental prototype.

TABLE I
ELECTRICAL AND CONTROL PARAMETERS OF EACH CONVERTER

BVCC$_1$ and BVCC$_2$		BCCC$_1$		BCCC$_2$	
Parameters	Values	Parameters	Values	Parameters	Values
$C_{\text{in},1}$, $C_{\text{in},2}$	850 μF	$C_{\text{in},3}$	100 μF	$C_{\text{in},4}$	100 μF
$R_{\text{C\_in},1}$, $R_{\text{C\_in},2}$	0.2 Ω	$R_{\text{C\_in},3}$	0.1 Ω	$R_{\text{C\_in},4}$	0.1 Ω
L_1, L_2	1.02 mH	L_3	200 μH	L_4	200 μH
$R_{\text{L},1}$, $R_{\text{L},2}$	0.1 Ω	$R_{\text{L},3}$	0.05 Ω	$R_{\text{L},4}$	0.05 Ω
C_1, C_2	200 μF	C_3	47 μF	C_4	47 μF
$R_{\text{C},1}$, $R_{\text{C},2}$	0.16 Ω	$R_{\text{C},3}$	0.1 Ω	$R_{\text{C},4}$	0.1 Ω
H_1, H_2	1/48	H_3	1/12	H_4	1/15
$k_{\text{p},1}$, $k_{\text{p},2}$	0.1	$k_{\text{p},3}$	1.7	$k_{\text{p},4}$	1.2
$k_{\text{i},1}$, $k_{\text{i},2}$	125	$k_{\text{i},3}$	200	$k_{\text{i},4}$	200
$v_{\text{o},1}$, $v_{\text{o},2}$	48 V	$v_{\text{o},3}$	12 V	$v_{\text{o},4}$	15 V

V. Case Study and Experimental Verification

In order to verify the correctness of the proposed BNIC, a dc distribution power system composed of four buck converters and its experimental prototype were built, as illustrated in Figs. 8 and 9, respectively. Notice that the input dc power, loads, auxiliary powers, and oscilloscope are not shown in Fig. 9. There are four nodes (n_1, n_2, n_3, n_4) and their voltages are v_1, v_2, v_3, and v_4, respectively. The lines impedance network includes three impedance $Z_{\text{line},1}$, $Z_{\text{line},2}$, and $Z_{\text{line},3}$. The switching frequency is 50 kHz. The input voltage of each BVCC is 80 V. The control is completed with DSP-TMS320F 28335.

The main electrical and control parameters of each converter are given in Table I. Each converter adopts the output-voltage-control mode. Here, for the xth buck converter, $C_{\text{in},x}$ and $R_{\text{Cin\_}x}$ are the input filter capacitance and its equivalent series resistance (ESR), respectively; L_x and $R_{\text{L},x}$ are the inductance and its ESR, respectively; C_x and $R_{\text{C},x}$ are the output filter capacitance and its ESR, respectively; H_x is the feedback coefficient; $k_{\text{p},x}$ and $k_{\text{i},x}$

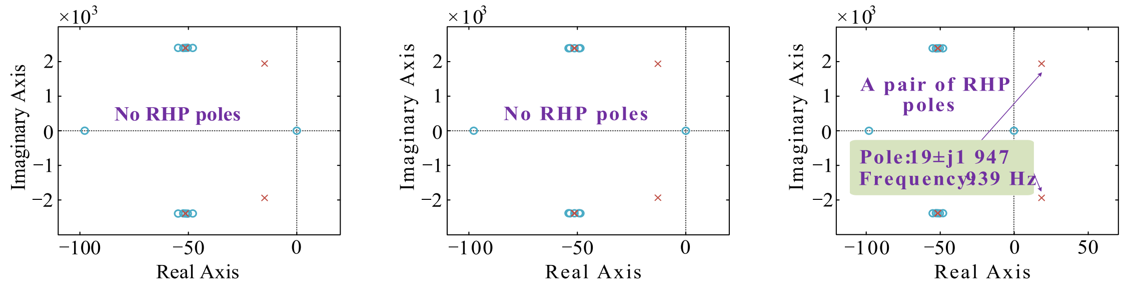

(a) (b) (c)

Fig. 10. Zero-pole-maps of $Z_{\mathrm{bus},1}$. (a) Case 1. (b) Case 2. (c) Case 3.

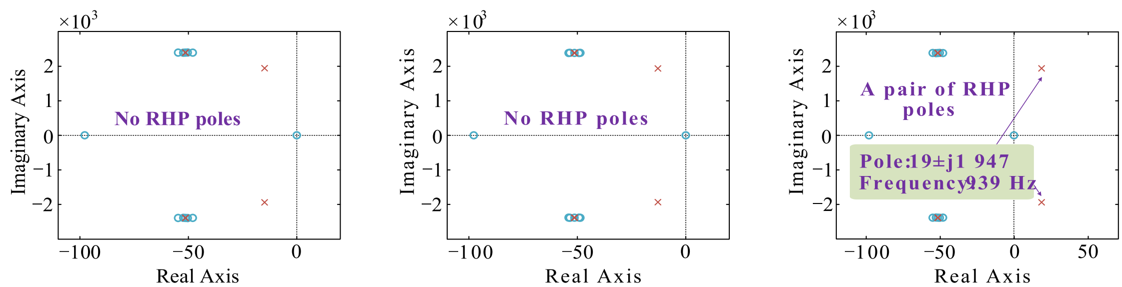

(a) (b) (c)

Fig. 11. Zero-pole-maps of $Z_{\mathrm{bus},2}$. (a) Case 1. (b) Case 2. (c) Case 3.

TABLE II
LOADS UNDER DIFFERENT CASES

Load resistance	Case 1	Case 2	Case 3
R_3	25 Ω	11.2 Ω	11.2 Ω
R_4	12 Ω	12 Ω	1.4 Ω

are the proportional and integral coefficients of the PI controller, respectively; $v_{\mathrm{o},x}$ and $i_{\mathrm{o},x}$ are the output voltage and current, respectively.

To analysis the system stability under different load power, three cases are set, as illustrated in Table II. Note that since BCCC_1 and BCCC_2 behave as CPLs, their input power can be changed by changing the values of their load resistances R_3 and R_4.

A. Lines Impedance Network is Considered

The line impedances are set as $Z_{\mathrm{line},1} = Z_{\mathrm{line},2} = Z_{\mathrm{line},3} = 0.22 + \mathrm{j}\, 2\pi \times 10^{-4}\ \Omega$. According to the Fig. 8, there are

$$\boldsymbol{Y}_{\mathrm{in}} = \mathrm{diag}(1,\ 1,\ -Y_{\mathrm{in},1},\ -Y_{\mathrm{in},2})$$

$$\boldsymbol{Z}_{\mathrm{o}} = \mathrm{diag}(Z_{\mathrm{o},1},\ Z_{\mathrm{o},2},\ -1,\ -1)$$

$$\boldsymbol{Y}_{\mathrm{net}} = \begin{bmatrix} Y_{\mathrm{line},1} & 0 & -Y_{\mathrm{line},1} & 0 \\ 0 & Y_{\mathrm{line},3} & 0 & -Y_{\mathrm{line},3} \\ -Y_{\mathrm{line},1} & 0 & Y_{\mathrm{line},1}+Y_{\mathrm{line},2} & -Y_{\mathrm{line},2} \\ 0 & -Y_{\mathrm{line},3} & -Y_{\mathrm{line},2} & Y_{\mathrm{line},2}+Y_{\mathrm{line},3} \end{bmatrix}. \tag{29}$$

Based on (16) and (29), combining with Tables I and II, the zero-pole-maps of four bus node impedances under different cases are shown in Figs. 10–13, respectively. Due to the size limitation, only the poles and zeros whose real parts are greater than –100 are given in this article. From Figs. 10 to 13, it can be seen that, under cases 1 and 2, each bus node impedance has no RHP poles, while they all have the same RHP poles under case 3, and the corresponding frequency is about 939 Hz. According to the proposed BNIC, the whole system is stable under cases 1 and 2, while it is unstable under case 3 and the system oscillation is expected to occur near 939 Hz. It should be pointed out that although we give the zero-pole-maps of four bus node impedances, the above conclusion can be obtained by *any* bus node impedance.

Besides, to verify the det($\boldsymbol{Y}_{\mathrm{in}} + \boldsymbol{Z}_{\mathrm{o}}\boldsymbol{Y}_{\mathrm{net}}$)-based stability criterion, the Nyquist curves of det($\boldsymbol{Y}_{\mathrm{in}} + \boldsymbol{Z}_{\mathrm{o}}\boldsymbol{Y}_{\mathrm{net}}$) under different cases are presented as Fig. 14. Notice that the Nyquist curves in this article are only shown for the frequencies from $\omega = 0$ to $+\infty$, this is because the other half corresponding to the frequency from $\omega = -\infty$ to 0 is not measurable in practical application, but is symmetric to the half shown. Therefore, the actual number N_{r} of encirclements around the origin (0, j0) should be doubled from the number obtained from the Fig. 14. According to [62] and [63], N_{r} can be obtained as

$$N_{\mathrm{r}} = 2(N_{+} - N_{-}) \tag{30}$$

where N_{+} is the positive crossing and N_{-} is the negative crossing. Their calculation methods are: when the Nyquist curve crosses the negative real axis on the left side of (0, j0) from top to bottom,

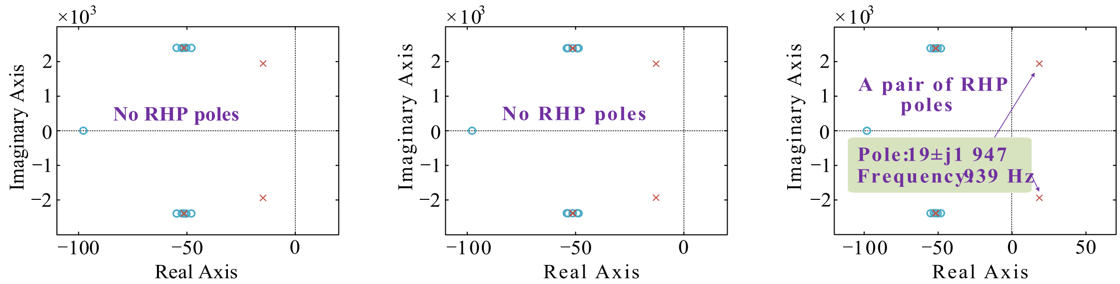

(a) (b) (c)

Fig. 12. Zero-pole-maps of $Z_{\mathrm{bus},3}$. (a) Case 1. (b) Case 2. (c) Case 3.

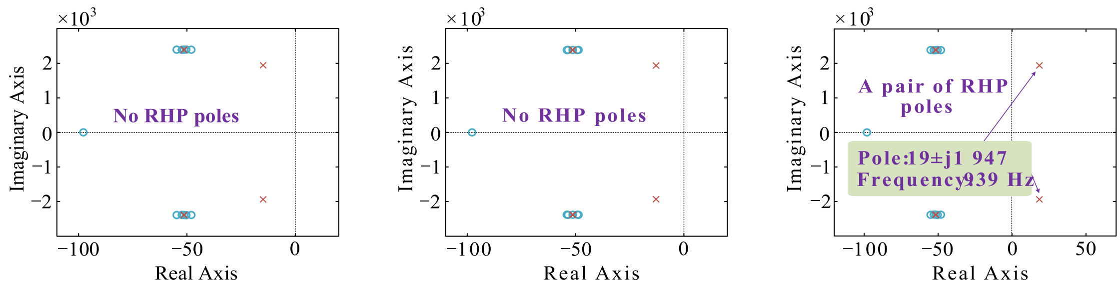

(a) (b) (c)

Fig. 13. Zero-pole-maps of $Z_{\mathrm{bus},4}$. (a) Case 1. (b) Case 2. (c) Case 3.

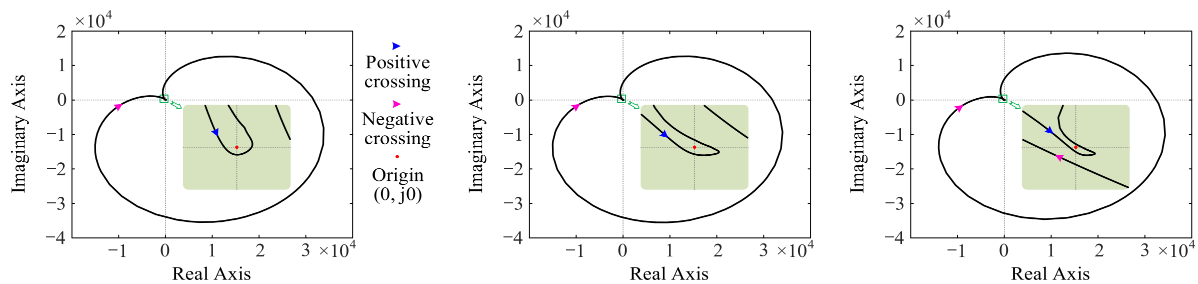

(a) (b) (c)

Fig. 14. Nyquist curves of $\det(\boldsymbol{Y}_{\mathrm{in}} + \boldsymbol{Z}_{\mathrm{o}}\boldsymbol{Y}_{\mathrm{net}})$. (a) Case 1. (b) Case 2. (c) Case 3.

it is one positive crossing; when it crosses from bottom to top, it is one negative crossing [62], [63]. Note that $N_{\mathrm{r}} > 0$ means the Nyquist curve surrounds (0, j0) anti-clockwise, while $N_{\mathrm{r}} < 0$ represents the Nyquist curve surrounds (0, j0) clockwise.

From the Fig. 14, it can be seen that, under cases 1 and 2, there is $N_{+} = N_{-} = 1$, that is, $N_{\mathrm{r}} = 0$; under case 3, there are $N_{+} = 1$ and $N_{-} = 2$, that is, $N_{\mathrm{r}} = -1$ and the Nyquist curve of $\det(\boldsymbol{Y}_{\mathrm{in}} + \boldsymbol{Z}_{\mathrm{o}}\boldsymbol{Y}_{\mathrm{net}})$ surrounds (0, j0) clockwise. Hence the whole system is stable under cases 1 and 2 while unstable under case 3, which is consistent with the analysis based on the proposed BNIC.

In order to illustrate the transient performance of the system, step change between each case is intentionally set. The system experimental waveforms are illustrated in Figs. 15 and 16, respectively. Here, the four node voltages (v_1, v_2, v_3, v_4), and the output voltages ($v_{\mathrm{o},3}$, $v_{\mathrm{o},4}$) and currents ($i_{\mathrm{o},3}$, $i_{\mathrm{o},4}$) of two BCCCs are shown. As aforementioned, the system will remain stable before and after the step changes from cases 1 to 2, while the system switches from stable state to unstable state when the step changes from cases 2 to 3. According to Figs. 15 and 16, the system is stable under both cases 1 and 2, but unstable and underdamped low-frequency oscillation under case 3. Furthermore, to obtain the system oscillation frequency, the bus voltage v_1 under case 3 is processed by the oscilloscope to conduct the fast Fourier transform (FFT) analysis. The results are shown in Fig. 17. It can be seen that the oscillation frequency of the experimental waveforms is about 949 Hz, which is basically the same as the analysis in Figs. 10–13. Due to component tolerances, the actual value of component parameters often deviates from the nominal value; therefore, the oscillation frequency error is acceptable.

In summary, the experimental results show that the stability analysis based on the proposed BNIC is feasible.

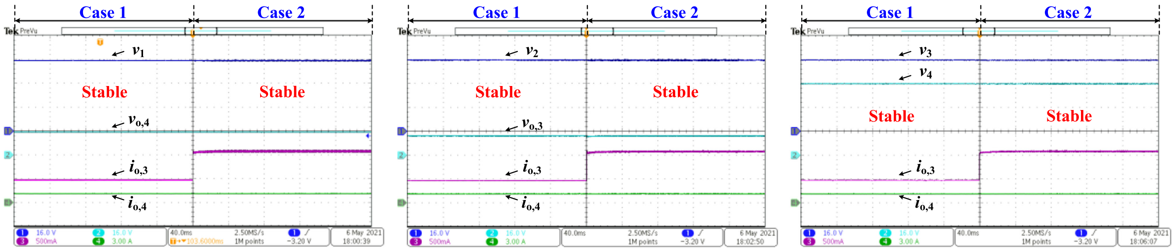

(a) (b) (c)

Fig. 15. Experimental waveforms from case 1 to case 2 when the lines impedance network is considered. (a) v_1, $v_{o,4}$, $i_{o,3}$, and $i_{o,4}$. (b) v_2, $v_{o,3}$, $i_{o,3}$, and $i_{o,4}$. (c) v_3, v_4, $i_{o,3}$, and $i_{o,4}$.

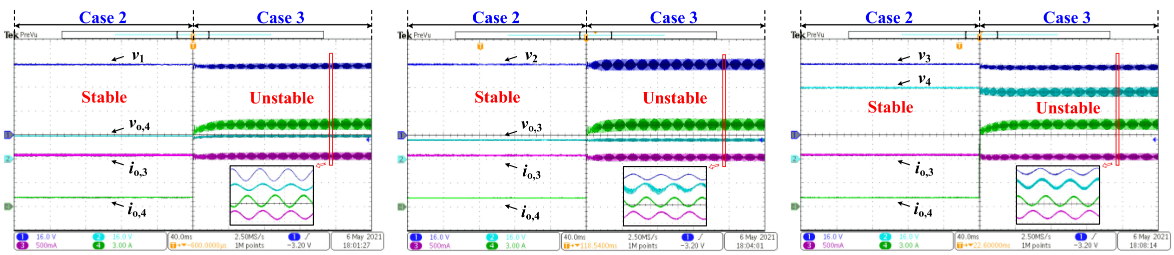

(a) (b) (c)

Fig. 16. Experimental waveforms from case 2 to case 3 when the lines impedance network is considered. (a) v_1, $v_{o,4}$, $i_{o,3}$, and $i_{o,4}$. (b) v_2, $v_{o,3}$, $i_{o,3}$, and $i_{o,4}$. (c) v_3, v_4, $i_{o,3}$, and $i_{o,4}$.

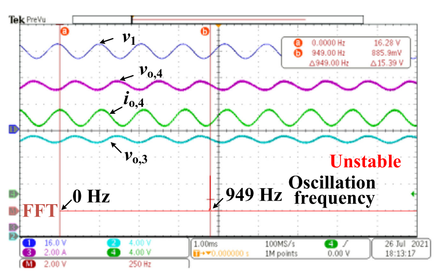

Fig. 17. FFT analysis of the bus voltage v_1 under case 3 when the lines impedance network is considered.

B. Lines Impedance Network is Ignored

In Fig. 8, the line impedance $Z_{\text{line},1}$, $Z_{\text{line},2}$, $Z_{\text{line},3}$ are all set to 0. Hence there is only one node on the bus and its voltage is $v_{\text{bus}} = v_1 = v_2 = v_3 = v_4$. Based on (23), the bus impedance can be expressed as

$$Z_{\text{bus}} = \frac{1}{1/Z_{o,1} + 1/Z_{o,2} + Y_{\text{in},1} + Y_{\text{in},2}}. \quad (31)$$

Combining with Tables I and II, the zero-pole-maps of Z_{bus} under three cases are shown in Fig. 18. Obviously, under case 1, Z_{bus} has no RHP poles, while it has a pair of RHP poles under cases 2 and 3, respectively. Accordingly, under cases 2 and 3, the system oscillation is expected to occur near 379 and 427 Hz, respectively. Notice that as shown in Fig. 18(b), the RHP poles are very close to the imaginary axis, which means the system will have a very small oscillation under case 2. According to the proposed BNIC, the whole system is stable only under case 1 and unstable under the other two cases.

The system experimental waveforms are illustrated in Figs. 19 and 20. Here, the bus voltages v_{bus}, and the output voltages ($v_{o,3}$, $v_{o,4}$) and currents ($i_{o,3}$, $i_{o,4}$) of two BCCCs are shown. As aforementioned, the system switches from stable state to unstable state when the step changes from cases 1 to 2, while the system remains unstable before and after the step changes from cases 2 to 3. According to Figs. 19 and 20, the system is stable under case 1, but unstable and underdamped low-frequency oscillation under both cases 2 and 3. What is more, the system oscillation amplitude under case 2 is very small. Furthermore, to obtain the system oscillation frequency, the bus voltage v_{bus} under cases 2 and 3 are processed by the oscilloscope to conduct the FFT analysis. The results are shown in Fig. 21. It can be seen that the oscillation frequencies are basically the same as the analysis in Fig 18. Therefore, the experimental results are also consistent with the stability analysis based on the proposed BNIC.

Compared with Figs. 15 and 19, it can be seen that under case 2, the system is stable when the line impedance network is considered, but it is unstable when the line impedance network is ignored. Therefore, the line impedance network should not be neglected when we discuss the stability of the geographically distributed system. Otherwise, it may lead to misjudgment.

Besides, in order to further verify the difference between the PBSC and the proposed BNIC, the bode plot of Z_{bus} under case 1 is given as an example, as shown in Fig. 22. According to the previous analysis and experiments, the system is stable under case 1. However, in Fig. 22, the phase angle of Z_{bus} is within the interval (90°, 135°) from 1 to 309 Hz. In other words, although the system does not meet $\text{Re}\{Z_{\text{bus}}(j\omega)\} \geq 0$ ($\forall\omega$), it is still

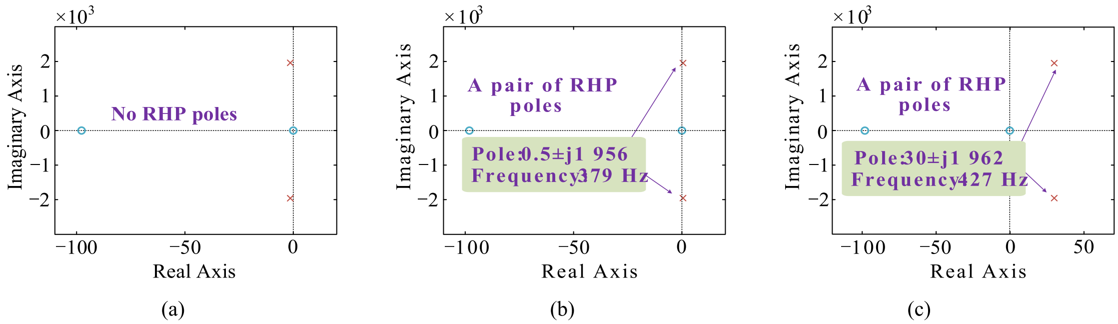

Fig. 18. Zero-pole-maps of $Z_{\rm bus}$. (a) Case 1. (b) Case 2. (c) Case 3.

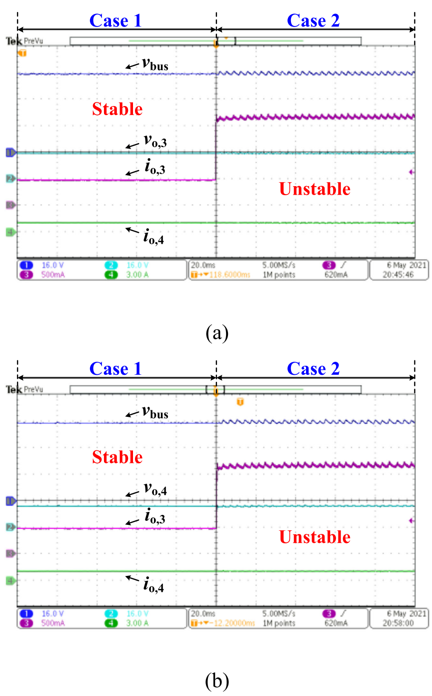

Fig. 19. Experimental waveforms from case 1 to case 2 when the lines impedance network is ignored. (a) $v_{\rm bus}$, $v_{\rm o,3}$, $i_{\rm o,3}$, and $i_{\rm o,4}$. (b) $v_{\rm bus}$, $v_{\rm o,4}$, $i_{\rm o,3}$, and $i_{\rm o,4}$.

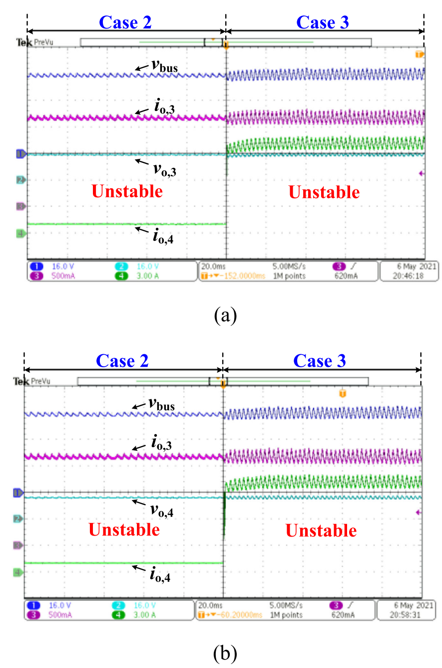

Fig. 20. Experimental waveforms from case 2 to case 3 when the lines impedance network is ignored. (a) $v_{\rm bus}$, $v_{\rm o,3}$, $i_{\rm o,3}$, and $i_{\rm o,4}$. (b) $v_{\rm bus}$, $v_{\rm o,4}$, $i_{\rm o,3}$, and $i_{\rm o,4}$.

stable. This example shows that the PBSC is not the necessary condition for system stability.

In summary, the above analysis and verification show that the proposed BNIC is a generic small-signal stability criterion for the dc distribution power system.

VI. Conclusion

In this article, the small-signal stability issues of the geographically distributed and centralized dc distribution power system are studied together in detail. First, the system small-signal model is established and the transfer function from each input disturbance to the bus voltage is derived. Then, a novel stability criterion, the BNIC, is proposed. According to the proposed BNIC, such a system is stable *if and only if* the bus impedance at any node does not have any RHP poles, which means the system stability can be evaluated by *any* bus node impedance. Compared with the existing stability criteria, the proposed BNIC is generic and suitable for wider application scenarios. Finally, the cases study and experimental results indicate that the proposed BNIC can effectively assess the stability of the dc distribution power system regardless of the line impedance network is considered or not.

Appendix

A. Measurement Method of Node Admittance Matrix of the Line Impedance Network

Assume that $y_{a,b}$ ($a, b = 1, 2, \ldots, r$) is the admittance in the ath row and bth column of $\boldsymbol{Y}_{\rm net}$. When $a = b$, $y_{b,b}$ is called self-admittance at node $\rm n_b$, otherwise $y_{a,b}$ ($a \neq b$) is called the mutual admittance between nodes $\rm n_a$ and $\rm n_b$ [64]. What's more, $\boldsymbol{Y}_{\rm net}$ is symmetric. When the line parameters cannot be obtained directly, the node admittance matrix $\boldsymbol{Y}_{\rm net}$ of the line impedance network can also be measured as shown in Fig. 23

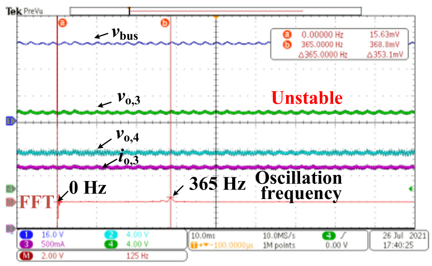

(a)

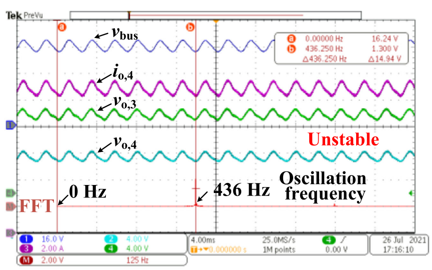

(b)

Fig. 21. FFT analysis of the bus voltage v_{bus}. (a) Case 2. (b) Case 3.

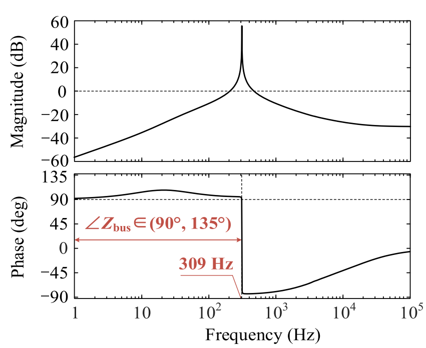

Fig. 22. Bode plot of Z_{bus} under case 1.

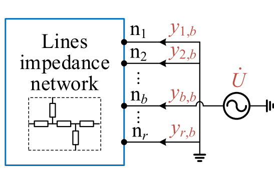

Fig. 23. Measurement method of $\boldsymbol{Y}_{\text{net}}$.

[65]. Here, all nodes except node n_b are grounded and $\dot{U}$ is the unit sine ac voltage. According to the above definition, $y_{b,b}$ is the current flowing into node n_b and $y_{a,b}$ is the current flowing into node n_a.

B. More Detailed Derivation About det($\boldsymbol{Y}_{\text{in}} + \boldsymbol{Z}_{\text{o}}\boldsymbol{Y}_{\text{net}}$)*-Based Stability Criterion and the Proposed BNIC*

Assume that the adjoint matrix adj($\boldsymbol{Y}_{\text{in}} + \boldsymbol{Z}_{\text{o}}\boldsymbol{Y}_{\text{net}}$) can be expressed as

$$\text{adj}\left(\boldsymbol{Y}_{\text{in}} + \boldsymbol{Z}_{\text{o}}\boldsymbol{Y}_{\text{net}}\right) = \begin{bmatrix} G_{1,1} & G_{1,2} & \cdots & G_{1,r} \\ G_{2,1} & G_{2,2} & \cdots & G_{2,r} \\ \vdots & \vdots & & \vdots \\ G_{r,1} & G_{r,2} & \cdots & G_{r,r} \end{bmatrix}. \quad \text{(A.1)}$$

Based on (12) and (A.1), there is

$$\left(\boldsymbol{Y}_{\text{in}} + \boldsymbol{Z}_{\text{o}}\boldsymbol{Y}_{\text{net}}\right)^{-1} = \begin{bmatrix} \frac{G_{1,1}}{\det(\boldsymbol{Y}_{\text{in}}+\boldsymbol{Z}_{\text{o}}\boldsymbol{Y}_{\text{net}})} & \frac{G_{1,2}}{\det(\boldsymbol{Y}_{\text{in}}+\boldsymbol{Z}_{\text{o}}\boldsymbol{Y}_{\text{net}})} & \cdots & \frac{G_{1,r}}{\det(\boldsymbol{Y}_{\text{in}}+\boldsymbol{Z}_{\text{o}}\boldsymbol{Y}_{\text{net}})} \\ \frac{G_{2,1}}{\det(\boldsymbol{Y}_{\text{in}}+\boldsymbol{Z}_{\text{o}}\boldsymbol{Y}_{\text{net}})} & \frac{G_{2,2}}{\det(\boldsymbol{Y}_{\text{in}}+\boldsymbol{Z}_{\text{o}}\boldsymbol{Y}_{\text{net}})} & \cdots & \frac{G_{2,r}}{\det(\boldsymbol{Y}_{\text{in}}+\boldsymbol{Z}_{\text{o}}\boldsymbol{Y}_{\text{net}})} \\ \vdots & \vdots & & \vdots \\ \frac{G_{r,1}}{\det(\boldsymbol{Y}_{\text{in}}+\boldsymbol{Z}_{\text{o}}\boldsymbol{Y}_{\text{net}})} & \frac{G_{r,2}}{\det(\boldsymbol{Y}_{\text{in}}+\boldsymbol{Z}_{\text{o}}\boldsymbol{Y}_{\text{net}})} & \cdots & \frac{G_{r,r}}{\det(\boldsymbol{Y}_{\text{in}}+\boldsymbol{Z}_{\text{o}}\boldsymbol{Y}_{\text{net}})} \end{bmatrix}. \quad \text{(A.2)}$$

Obviously, compared with (A.2), the determinant det($\boldsymbol{Y}_{\text{in}} + \boldsymbol{Z}_{\text{o}}\boldsymbol{Y}_{\text{net}}$) has less impedance calculation. Besides, when each BVCC and BCCC are stable individually, based on the proposed *lemma*, $G_{a,b}$ has no RHP poles. Therefore, each transfer function in (A.2) have the same denominator for discussing its RHP poles, that is, det($\boldsymbol{Y}_{\text{in}} + \boldsymbol{Z}_{\text{o}}\boldsymbol{Y}_{\text{net}}$). In other words, the system stability can be simply judged by det($\boldsymbol{Y}_{\text{in}} + \boldsymbol{Z}_{\text{o}}\boldsymbol{Y}_{\text{net}}$).

According to (16), $Z_{\text{bus},\alpha}$ is the element in αth row and αth column of the matrix $(\boldsymbol{Y}_{\text{in}} + \boldsymbol{Z}_{\text{o}}\boldsymbol{Y}_{\text{net}})^{-1}\boldsymbol{Z}_{\text{o}}$. Therefore, $Z_{\text{bus},\alpha}$ can be rewritten as

$$Z_{\text{bus},\alpha} = \begin{cases} \frac{G_{\alpha,\alpha}}{\det(\boldsymbol{Y}_{\text{in}}+\boldsymbol{Z}_{\text{o}}\boldsymbol{Y}_{\text{net}})} Z_{\text{o},\alpha}, & \alpha \le k \\ -\frac{G_{\alpha,\alpha}}{\det(\boldsymbol{Y}_{\text{in}}+\boldsymbol{Z}_{\text{o}}\boldsymbol{Y}_{\text{net}})}, & \alpha > k. \end{cases} \quad \text{(A.3)}$$

According to the definition of the adjoint matrix, for each transfer function $G_{a,b}$ in adj($\boldsymbol{Y}_{\text{in}} + \boldsymbol{Z}_{\text{o}}\boldsymbol{Y}_{\text{net}}$), the calculation complexity is the same. Compared with (A.2) and (A.3), the impedance calculation complexity of $Z_{\text{bus},\alpha}$ and each transfer function in $(\boldsymbol{Y}_{\text{in}} + \boldsymbol{Z}_{\text{o}}\boldsymbol{Y}_{\text{net}})^{-1}$ is almost the same. Therefore, $Z_{\text{bus},\alpha}$ also has less impedance calculation than $(\boldsymbol{Y}_{\text{in}} + \boldsymbol{Z}_{\text{o}}\boldsymbol{Y}_{\text{net}})^{-1}$. In other words, the proposed stability criteria is more concise than the criterion based on CCM. Meanwhile, no matter at which node (or what value α takes), $Z_{\text{bus},\alpha}$ has the same denominator for discussing its RHP poles, that is, det($\boldsymbol{Y}_{\text{in}} + \boldsymbol{Z}_{\text{o}}\boldsymbol{Y}_{\text{net}}$). Hence, the system stability can also be evaluated by the bus impedance at *any* node.

C. Comparison With the Existing Determinant-Based Stability Criteria

1) The existing determinant-based stability criteria are completely equivalent to the proposed det($\boldsymbol{Y}_{\text{in}} + \boldsymbol{Z}_{\text{o}}\boldsymbol{Y}_{\text{net}}$)-based stability criterion.

First, it should be pointed out that, according to the different system modeling methods and the matrix or determinant transformation rules, there are many ways to define and choose the determinant for the stability analysis of dc distribution power system. For example, based on the model established in Section III-A, there are two classical determinant-based stability criteria can also be derived as follows.

Determinant-based stability criterion 1: According to [52] and (3), we can define a determinant det($\boldsymbol{Y} + \boldsymbol{Y}_{\text{net}}$)-based stability criterion, that is, the system is stable *if and only if* det($\boldsymbol{Y} + \boldsymbol{Y}_{\text{net}}$) has no RHP zeros. Note that the matrix $\boldsymbol{Y} + \boldsymbol{Y}_{\text{net}}$ is the nodal admittance matrix according to circuit theory [60], and the det($\boldsymbol{Y} + \boldsymbol{Y}_{\text{net}}$)-based stability criterion is the same as the determinant det($\boldsymbol{Y}_{\text{node}}$)-based stability criterion proposed in [52]–[54].

Determinant-based stability criterion 2: According to the matrix or determinant transformation rules, there is

$$\begin{aligned}\det(\boldsymbol{Y}+\boldsymbol{Y}_{\text{net}}) &= \det((\boldsymbol{Y}+\boldsymbol{Y}_{\text{net}})\boldsymbol{Y}_{\text{net}}^{-1}\boldsymbol{Y}_{\text{net}}) \\ &= \det((\boldsymbol{Y}+\boldsymbol{Y}_{\text{net}})\boldsymbol{Y}_{\text{net}}^{-1})\cdot\det(\boldsymbol{Y}_{\text{net}}) \\ &= \det(\boldsymbol{E}+\boldsymbol{L})\cdot\det(\boldsymbol{Y}_{\text{net}}) \qquad \text{(A.4)}\end{aligned}$$

where $\boldsymbol{E}$ is the identity matrix, $\boldsymbol{L} = \boldsymbol{Y}\boldsymbol{Z}_{\text{net}}$ is the well-known return-ratio matrix, and $\boldsymbol{Z}_{\text{net}} = \boldsymbol{Y}_{\text{net}}^{-1}$.

Therefore, we can also define a determinant det($\boldsymbol{E} + \boldsymbol{L}$)-based stability criterion, that is, the system is stable *if and only if* det($\boldsymbol{E} + \boldsymbol{L}$) has no RHP zeros. This criterion is similar as the criteria proposed in [55] and [56].

In order to prove that det($\boldsymbol{Y} + \boldsymbol{Y}_{\text{net}}$)-based and det($\boldsymbol{E} + \boldsymbol{L}$)-based stability criteria are completely equivalent to the proposed det($\boldsymbol{Y}_{\text{in}} + \boldsymbol{Z}_{\text{o}}\boldsymbol{Y}_{\text{net}}$)-based stability criterion, we need to prove that these determinants have the same RHP zeros. Based on the matrix and determinant transformation rules, combined with (7) and (A.4), the RHP zeros of det($\boldsymbol{Y} + \boldsymbol{Y}_{\text{net}}$) and det($\boldsymbol{E} + \boldsymbol{L}$) can be calculated by

$$\begin{aligned}\mathbb{Z}\left[\det(\boldsymbol{Y}+\boldsymbol{Y}_{\text{net}})\right] &= \mathbb{Z}\left[\det(\boldsymbol{Z}_{\text{o}}^{-1}\boldsymbol{Y}_{\text{in}}+\boldsymbol{Y}_{\text{net}})\right] \\ &= \mathbb{Z}\left[\det(\boldsymbol{Z}_{\text{o}}^{-1}\boldsymbol{Z}_{\text{o}}(\boldsymbol{Z}_{\text{o}}^{-1}\boldsymbol{Y}_{\text{in}}+\boldsymbol{Y}_{\text{net}}))\right] \\ &= \mathbb{Z}\left[\det(\boldsymbol{Y}_{\text{in}}+\boldsymbol{Z}_{\text{o}}\boldsymbol{Y}_{\text{net}})/\det(\boldsymbol{Z}_{\text{o}})\right] \\ &= \mathbb{Z}\left[\det(\boldsymbol{Y}_{\text{in}}+\boldsymbol{Z}_{\text{o}}\boldsymbol{Y}_{\text{net}})\right]+\mathbb{P}\left[\det(\boldsymbol{Z}_{\text{o}})\right] \qquad \text{(A.5)}\end{aligned}$$

$$\begin{aligned}\mathbb{Z}\left[\det(\boldsymbol{E}+\boldsymbol{L})\right] &= \mathbb{Z}\left[\det(\boldsymbol{E}+\boldsymbol{Y}\boldsymbol{Y}_{\text{net}}^{-1})\right] \\ &= \mathbb{Z}\left[\det((\boldsymbol{E}+\boldsymbol{Y}\boldsymbol{Y}_{\text{net}}^{-1})\boldsymbol{Y}_{\text{net}}\boldsymbol{Y}_{\text{net}}^{-1})\right] \\ &= \mathbb{Z}\left[\det(\boldsymbol{Y}+\boldsymbol{Y}_{\text{net}})/\det(\boldsymbol{Y}_{\text{net}})\right] \\ &= \mathbb{Z}\left[\det(\boldsymbol{Y}+\boldsymbol{Y}_{\text{net}})\right]+\mathbb{P}\left[\det(\boldsymbol{Y}_{\text{net}})\right] \qquad \text{(A.6)}\end{aligned}$$

where $\mathbb{Z}$ denotes the number of RHP zeros, and $\mathbb{P}$ denotes the number of RHP poles.

Based on (5), there are

$$\begin{aligned}\det(\boldsymbol{Z}_{\text{o}}) &= (-1)^m Z_{\text{o},1}\cdots Z_{\text{o},k}, \\ \det(\boldsymbol{Y}_{\text{in}}) &= (-1)^m Y_{\text{in},1}\ \cdots Y_{\text{in},m}. \qquad \text{(A.7)}\end{aligned}$$

Because any converter is stable individually, each transfer function element in both $\boldsymbol{Y}_{\text{in}}$ and $\boldsymbol{Z}_{\text{o}}$ has no RHP poles. Therefore, both det($\boldsymbol{Y}_{\text{in}}$) and det($\boldsymbol{Z}_{\text{o}}$) have no RHP poles, that is

$$\mathbb{P}\left[\det(\boldsymbol{Z}_{\text{o}})\right]=0,\ \mathbb{P}\left[\det(\boldsymbol{Y}_{\text{in}})\right]=0. \qquad \text{(A.8)}$$

Besides, as mentioned in Section III-B, $\boldsymbol{Y}_{\text{net}}$ has no RHP poles, furthermore, det($\boldsymbol{Y}_{\text{net}}$) has no RHP zeros and poles, that is

$$\mathbb{Z}\left[\det(\boldsymbol{Y}_{\text{net}})\right]=0,\ \mathbb{P}\left[\det(\boldsymbol{Y}_{\text{net}})\right]=0. \qquad \text{(A.9)}$$

Combined with (A.5), (A.6), (A.8), and (A.9), we can obtain that

$$\begin{aligned}\mathbb{Z}\left[\det(\boldsymbol{Y}+\boldsymbol{Y}_{\text{net}})\right] &= \mathbb{Z}\left[\det(\boldsymbol{Y}_{\text{in}}+\boldsymbol{Z}_{\text{o}}\boldsymbol{Y}_{\text{net}})\right] \\ &= \mathbb{Z}\left[\det(\boldsymbol{E}+\boldsymbol{L})\right]. \qquad \text{(A.10)}\end{aligned}$$

From (A.10), it can be seen that determinants det($\boldsymbol{Y} + \boldsymbol{Y}_{\text{net}}$), det($\boldsymbol{E} + \boldsymbol{L}$), and det($\boldsymbol{Y}_{\text{in}} + \boldsymbol{Z}_{\text{o}}\boldsymbol{Y}_{\text{net}}$) have the same RHP zeros. Therefore, the nodal admittance matrix-based and return-ratio matrix-based determinant stability criteria are completely equivalent to the proposed det($\boldsymbol{Y}_{\text{in}} + \boldsymbol{Z}_{\text{o}}\boldsymbol{Y}_{\text{net}}$)-based stability criterion. In other words, the dc distribution power system is stable *if and only if* det($\boldsymbol{Y} + \boldsymbol{Y}_{\text{net}}$) or det($\boldsymbol{E} + \boldsymbol{L}$) or det($\boldsymbol{Y}_{\text{in}} + \boldsymbol{Z}_{\text{o}}\boldsymbol{Y}_{\text{net}}$) has no RHP zeros.

Notice that [53] proved that nodal admittance matrix-based and loop impedance matrix-based determinant stability criteria are also completely equivalent, so the proposed det($\boldsymbol{Y}_{\text{in}} + \boldsymbol{Z}_{\text{o}}\boldsymbol{Y}_{\text{net}}$)-based stability criterion is completely equivalent to all the existing determinant-based stability criteria.

2) The proposed det($\boldsymbol{Y}_{\text{in}} + \boldsymbol{Z}_{\text{o}}\boldsymbol{Y}_{\text{net}}$)-based stability criterion is more generic and has wider application scenarios.

According to the above analysis, in order to assess the system stability, the RHP zeros of these determinants should be determined. For this purpose, we can model each converter and the line impedance network. However, this transfer function modeling method is invalid for the "black box" systems because the detailed circuit and control parameters are unknown and only the impedance frequency response can be measured. According to Cauchy's argument principle and the Nyquist criterion, when a transfer function has no RHP poles, its RHP zeros can be evaluated by its Nyquist curve or frequency response curve. Therefore, a determinant-based stability criterion will have wider application scenarios if it does not have RHP poles for any system. According to the proof and analysis in Section III-B of this article, det($\boldsymbol{Y}_{\text{in}} + \boldsymbol{Z}_{\text{o}}\boldsymbol{Y}_{\text{net}}$) is suitable for any "black box" system because it has no RHP poles once each converter operates stably individually. While the other determinants may have RHP poles in some case even if each converter is stable individually. The specific proof is as follows:

Based on (A.5) and (A.6), there are

$$\begin{aligned}\mathbb{P}\left[\det(\boldsymbol{Y}+\boldsymbol{Y}_{\text{net}})\right] &= \mathbb{P}\left[\det(\boldsymbol{Y}_{\text{in}}+\boldsymbol{Z}_{\text{o}}\boldsymbol{Y}_{\text{net}})/\det(\boldsymbol{Z}_{\text{o}})\right] \\ &= \mathbb{P}\left[\det(\boldsymbol{Y}_{\text{in}}+\boldsymbol{Z}_{\text{o}}\boldsymbol{Y}_{\text{net}})\right]+\mathbb{Z}\left[\det(\boldsymbol{Z}_{\text{o}})\right] \qquad \text{(A.11)}\end{aligned}$$

$$\begin{aligned}\mathbb{P}\left[\det(\boldsymbol{E}+\boldsymbol{L})\right] &= \mathbb{P}\left[\det(\boldsymbol{Y}+\boldsymbol{Y}_{\text{net}})/\det(\boldsymbol{Y}_{\text{net}})\right] \\ &= \mathbb{P}\left[\det(\boldsymbol{Y}+\boldsymbol{Y}_{\text{net}})\right]+\mathbb{Z}\left[\det(\boldsymbol{Y}_{\text{net}})\right]. \qquad \text{(A.12)}\end{aligned}$$

Because there is

$$\mathbb{P}\left[\det(\boldsymbol{Y}_{\text{in}}+\boldsymbol{Z}_{\text{o}}\boldsymbol{Y}_{\text{net}})\right]=0. \qquad \text{(A.13)}$$

Substituting (A.13) into (A.11) and (A.12), and combined with (A.7) and (A.9), there are

$$\begin{aligned}\mathbb{P}\left[\det(\boldsymbol{Y}+\boldsymbol{Y}_{\text{net}})\right] &= \mathbb{Z}\left[\det(\boldsymbol{Z}_{\text{o}})\right] \\ &= \mathbb{Z}\left[Z_{\text{o},1}\right]+\mathbb{Z}\left[Z_{\text{o},2}\right]+\cdots+\mathbb{Z}\left[Z_{\text{o},k}\right] \qquad \text{(A.14)}\end{aligned}$$

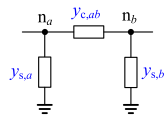

Fig. 24. Cross-line-admittance and self-line-admittance of the nodes.

$$\mathbb{P}\left[\det(\boldsymbol{E}+\boldsymbol{L})\right] = \mathbb{Z}\left[Z_{o,1}\right] + \mathbb{Z}\left[Z_{o,2}\right] + \cdots + \mathbb{Z}\left[Z_{o,k}\right]. \tag{A.15}$$

According to [31], there may be some RHP zeros in $Z_{o,k}$ although the BVCC$_k$ is stable individually; and there may be some RHP zeros in $Y_{in,m}$ even if the BCCC$_m$ is stable individually. The most typical example is the nonminimum-phase converter, such as a boost converter. Once there is a nonminimum-phase BVCC$_k$ in the system, there will be

$$\mathbb{Z}\left[Z_{o,k}\right] \neq 0. \tag{A.16}$$

Combined with (A.14) to (A.16), there are

$$\mathbb{P}\left[\det(\boldsymbol{Y}+\boldsymbol{Y}_{net})\right] \neq 0,\ \mathbb{P}\left[\det(\boldsymbol{E}+\boldsymbol{L})\right] \neq 0. \tag{A.17}$$

In other words, these determinants may have RHP poles and cannot be directly applied for any "black box" system.

Besides, when there is at least one non-minimum-phase BCCC, the loop impedance matrix-based determinant also have RHP poles, that is because the input impedance $1/Y_{in,m}$ of BCCC$_m$ will exist in some transfer function elements of this loop impedance matrix according to circuit theory [60], and $1/Y_{in,m}$ may have RHP poles.

In summary, the proposed det($\boldsymbol{Y}_{in} + \boldsymbol{Z}_o\boldsymbol{Y}_{net}$)-based stability criterion is a better choice and more generic.

D. Proof of (23) Derived From (16)

According to Fig. 4, there is

$$\hat{i}_{bus} = \boldsymbol{\xi}(\hat{i}_\alpha \boldsymbol{\eta}^T). \tag{A.18}$$

Substituting (17), (18), and (A.18) into (13), there is

$$\boldsymbol{\xi}\hat{i}_\alpha\boldsymbol{\eta}^T = \boldsymbol{\xi}(\boldsymbol{Y}+\boldsymbol{Y}_{net})\boldsymbol{\xi}^T\hat{v}_{bus}. \tag{A.19}$$

Hence, the bus impedance Z_{bus} can be expressed as

$$Z_{bus} = \frac{\hat{v}_{bus}}{\hat{i}_{bus}} = \frac{\boldsymbol{\xi}\boldsymbol{\eta}^T}{\boldsymbol{\xi}(\boldsymbol{Y}+\boldsymbol{Y}_{net})\boldsymbol{\xi}^T} = \left(\sum_{p=1}^{k} Y_{o,p} + \sum_{q=1}^{m} Y_{in,q}\right)^{-1} \tag{A.20}$$

which is consistent with (23).

E. Non-Generality Analysis of det($\boldsymbol{Y}_{in} + \boldsymbol{Z}_o\boldsymbol{Y}_{net}$)*-Based Stability Criterion*

For the dc distribution power system without line impedance network, there is only one equivalent node on the whole bus, in other words, the concepts of the transfer function matrix and determinant do not exist. Specifically, as shown in Fig. 24, the cross-line-admittance ($y_{c,ab}$) between two connected nodes is ∞ and the self-line-admittance ($y_{s,x}$ or $y_{s,y}$) of each node is 0. Therefore, each transfer function element of $\boldsymbol{Y}_{net}$ is 0 or ∞. Furthermore, there may be det($\boldsymbol{Y}_{in} + \boldsymbol{Z}_o\boldsymbol{Y}_{net}$) $= \infty$ and $G_{a,b} = \infty$, which means the stability criterion based on det($\boldsymbol{Y}_{in} + \boldsymbol{Z}_o\boldsymbol{Y}_{net}$) or (8) may not be utilized directly in the system without considering line impedance network.

ACKNOWLEDGMENT

The authors would like to thank all reviewers for their valuable suggestions and comments, which have helped the authors significantly improve this article.

REFERENCES

[1] A. Khan, M. Hosseinzadehtaher, M. B. Shadmand, S. Bayhan, and H. Abu-Rub, "On the stability of the power electronics-dominated grid: A new energy paradigm," *IEEE Ind. Electron. Mag.*, vol. 14, no. 4, pp. 65–78, Dec. 2020.

[2] M. G. Taul, X. Wang, P. Davari, and F. Blaabjerg, "Reduced-order and aggregated modeling of large-signal synchronization stability for multiconverter systems," *IEEE J. Emerg. Sel. Topics Power Electron.*, vol. 9, no. 3, pp. 3150–3165, Jun. 2021.

[3] X. Chen, Q. Hu, Q. Shi, X. Quan, Z. Wu, and F. Li, "Residential HVAC aggregation based on risk-averse multi-armed bandit learning for secondary frequency regulation," *J. Mod. Power Syst. Clean Energy*, vol. 8, no. 6, pp. 1160–1167, Nov. 2020.

[4] P. Pan *et al.*, "An impedance-based stability assessment methodology for DC distribution power system with multivoltage levels," *IEEE Trans. Power Electron.*, vol. 35, no. 4, pp. 4033–4047, Apr. 2020.

[5] S. Singh, A. R. Gautam, and D. Fulwani, "Constant power loads and their effects in DC distributed power systems: A review," *Renewable Sustain. Energy Rev.*, vol. 72, pp. 407–421, May 2017.

[6] H. Abdollahi, S. Arrua, T. Roinila, and E. Santi, "A novel DC power distribution system stabilization method based on adaptive resonance-enhanced voltage controller," *IEEE Trans. Ind. Electron.*, vol. 66, no. 7, pp. 5653–5662, Jul. 2019.

[7] J. Nie, Z. Zhao, L. Yuan, R. Duan, B. Shi, and L. Jin, "An energy balance active disturbance rejection control for improving converter stability while maintaining fast dynamic performance," *IEEE Trans. Power Electron.*, vol. 35, no. 11, pp. 11304–11309, Nov. 2020.

[8] H. Mu *et al.*, "Impedance-based stability analysis methods for DC distribution power system with multivoltage levels," *IEEE Trans. Power Electron.*, vol. 36, no. 8, pp. 9193–9208, Aug. 2021.

[9] Q. Peng, Y. Yang, T. Liu, and F. Blaabjerg, "Coordination of virtual inertia control and frequency damping in PV systems for optimal frequency support," *CPSS Trans. Power Electron. Appl.*, vol. 5, no. 4, pp. 305–316, Dec. 2020.

[10] X. Zhang, Q.-C. Zhong, V. Kadirkamanathan, J. He, and J. Huang, "Source-side series-virtual-impedance control to improve the cascaded system stability and the dynamic performance of its source converter," *IEEE Trans. Power Electron.*, vol. 34, no. 6, pp. 5854–5866, Jun. 2019.

[11] A. Khodamoradi, H. Abdollahi, E. Santi, and P. Mattavelli, "A loop gain-based technique for online bus impedance estimation and damping in DC microgrids," *IEEE Trans. Power Electron.*, vol. 36, no. 8, pp. 9648–9658, Aug. 2021.

[12] H. Liu, W. Guo, D. Cheng, Y. Wang, and M. Wang, "Stability and bifurcation analysis of DC microgrid with multiple droop control sources and loads," *IEEE Trans. Power Electron.*, vol. 36, no. 2, pp. 2361–2372, Feb. 2021.

[13] Y.-C. Jeung, D.-C. Lee, T. Dragicevic, and F. Blaabjerg, "Design of passivity-based damping controller for suppressing power oscillations in DC microgrids," *IEEE Trans. Power Electron.*, vol. 36, no. 4, pp. 4016–4028, Apr. 2021.

[14] M. Kabalan, P. Singh, and D. Niebur, "Large signal Lyapunov-based stability studies in microgrids: A review," *IEEE Trans. Smart Grid*, vol. 8, no. 5, pp. 2287–2295, Sep. 2017.

[15] W. Xie, M. Han, W. Cao, J. M. Guerrero, and J. C. Vasquez, "System-level large-signal stability analysis of droop-controlled DC microgrids," *IEEE Trans. Power Electron.*, vol. 36, no. 4, pp. 4224–4236, Apr. 2021.

[16] F. Chang, X. Cui, M. Wang, W. Su, and A. Q. Huang, "Large-signal stability criteria in DC power grids with distributed-controlled converters and constant power loads," *IEEE Trans. Smart Grid*, vol. 11, no. 6, pp. 5273–5287, Nov. 2020.

[17] J. Jiang *et al.*, "A conservatism-free large signal stability analysis method for DC microgrid based on mixed potential theory," *IEEE Trans. Power Electron.*, vol. 34, no. 11, pp. 11342–11351, Nov. 2019.

[18] H. Zheng, L. Zhou, P. Sun, and W. Lu, "Large-signal stability analysis for VSC-HVDC systems based on mixed potential theory," *IEEE Trans. Power Del.*, vol. 35, no. 4, pp. 1939–1948, Aug. 2020.

[19] W. Du, J. Zhang, Y. Zhang, and Z. Qian, “Stability criterion for cascaded system with constant power load,” *IEEE Trans. Power Electron.*, vol. 28, no. 4, pp. 1843–1851, Apr. 2013.

[20] J. Sun, “Small-signal methods for AC distributed power systems–A review,” *IEEE Trans. Power Electron.*, vol. 24, no. 11, pp. 2545–2554, Nov. 2009.

[21] Z. Xie, W. Wu, Y. Chen, and W. Gon, “Admittance-based stability comparative analysis of grid-connected inverters with direct power control and closed-loop current control,” *IEEE Trans. Ind. Electron.*, vol. 68, no. 9, pp. 8333–8344, Nov. 2021.

[22] Z. Huang, S. Wong, and C. K. Tse, “Revisiting stability criteria for DC power distribution systems based on power balance,” *CPSS Trans. Power Electron. Appl.*, vol. 2, no. 1, pp. 76–85, Apr. 2017.

[23] X. Wang, F. Blaabjerg, and W. Wu, “Modeling and analysis of harmonic stability in an AC power-electronics-based power system,” *IEEE Trans. Power Electron.*, vol. 29, no. 12, pp. 6421–6432, Dec. 2014.

[24] M. Amin and M. Molinas, “Small-signal stability assessment of power electronics based power systems: A discussion of impedance- and eigenvalue-based methods,” *IEEE Trans. Ind. Appl.*, vol. 53, no. 5, pp. 5014–5030, Sep. 2017.

[25] H. Zhang, M. Mehrabankhomartash, M. Saeedifard, Y. Zou, Y. Meng, and X. Wang, “Impedance analysis and stabilization of point-to-point HVDC systems based on a hybrid AC–DC impedance model,” *IEEE Trans. Ind. Electron.*, vol. 68, no. 4, pp. 3224–3238, Apr. 2021.

[26] L. Xiong *et al.*, “Static synchronous generator model: A new perspective to investigate dynamic characteristics and stability issues of grid-tied PWM inverter,” *IEEE Trans. Power Electron.*, vol. 31, no. 9, pp. 6264–6280, Sep. 2016.

[27] B. Liang, J. He, Y. W. Li, P. Guo, and C. Wang, “Aggregated-impedance-based stability analysis for a parallel-converter system considering the coupling effect of voltage feedforward control and reactive power injection,” *IEEE Trans. Power Electron.*, vol. 36, no. 5, pp. 5954–5970, May 2021.

[28] X. Feng, J. Liu, and F. C. Lee, “Impedance specifications for stable DC distributed power systems,” *IEEE Trans. Power Electron.*, vol. 17, no. 2, pp. 157–162, Mar. 2002.

[29] J. Lyu, X. Zhang, X. Cai, and M. Molinas, “Harmonic state-space based small-signal impedance modeling of a modular multilevel converter with consideration of internal harmonic dynamics,” *IEEE Trans. Power Electron.*, vol. 34, no. 3, pp. 2134–2148, Mar. 2019.

[30] H. Zhang, M. Mehrabankhomartash, M. Saeedifard, Y. Zou, Y. Meng, and X. Wang, “Impedance analysis and stabilization of point-to-point HVDC systems based on a hybrid AC–DC impedance model,” *IEEE Trans. Ind. Electron.*, vol. 68, no. 4, pp. 3224–3238, Apr. 2021.

[31] Y. Liao and X. Wang, “Impedance-based stability analysis for interconnected converter systems with open-loop RHP poles,” *IEEE Trans. Power Electron.*, vol. 35, no. 4, pp. 4388–4397, Apr. 2020.

[32] R. D. Middlebrook, “Input filter considerations in design and application of switching regulators,” in *Proc. IEEE Ind. Appl. Soc. Annu. Meeting*, 1976, pp. 366–382.

[33] A. Riccobono and E. Santi, “Comprehensive review of stability criteria for DC power distribution systems,” *IEEE Trans. Ind. Appl.*, vol. 50, no. 5, pp. 3525–3535, Sep. 2014.

[34] M. Leng *et al.*, “Impedance-based stability evaluation for multibus DC microgrid without constraints on subsystems,” *IEEE Trans. Power Electron.*, vol. 37, no. 1, pp. 932–943, Jan. 2022.

[35] J. Sun, “Impedance-based stability criterion for grid-connected inverters,” *IEEE Trans. Power Electron.*, vol. 26, no. 11, pp. 3075–3078, Nov. 2011.

[36] X. Zhang, X. Ruan, and C. K. Tse, “Impedance-based local stability criterion for DC distributed power systems,” *IEEE Trans. Circuits Syst. I, Reg. Papers*, vol. 62, no. 3, pp. 916–925, Mar. 2015.

[37] Q.-C. Zhong and X. Zhang, “Impedance-sum stability criterion for power electronic systems with two converters/sources,” *IEEE Access*, vol. 7, pp. 21254–21265, 2019.

[38] F. Liu, J. Liu, H. Zhang, and D. Xue, “Stability issues of z + z type cascade system in hybrid energy storage system (HESS),” *IEEE Trans. Power Electron.*, vol. 29, no. 11, pp. 5846–5859, Nov. 2014.

[39] W. Cao, K. Liu, S. Wang, H. Kang, D. Fan, and J. Zhao, “Harmonic stability analysis for multi-parallel inverter-based grid-connected renewable power system using global admittance,” *Energies*, vol. 12, no. 14, Jul. 2019, Art. no. 2687.

[40] A. Riccobono and E. Santi, “A novel passivity-based stability criterion (PBSC) for switching converter DC distribution systems,” in *Proc. 27th Annu . IEEE Appl. Power Electron. Conf. Expo.*, Orlando, FL, USA, 2012, pp. 2560–2567.

[41] Y. Li *et al.*, “Stability analysis and location optimization method for multiconverter power systems based on nodal admittance matrix,” *IEEE J. Emerg. Sel. Topics Power Electron.*, vol. 9, no. 1, pp. 529–538, Feb. 2021.

[42] N. Pogaku, M. Prodanovic, and T. C. Green, “Modeling, analysis and testing of an inverter-based microgrid,” *IEEE Trans. Power Electron.*,vol. 22, no. 2, pp. 613–625, Mar. 2007.

[43] E. Ebrahimzadeh, F. Blaabjerg, X. Wang, and C. L. Bak, “Harmonic stability and resonance analysis in large PMSG-based wind power plants,” *IEEE Trans. Sustain. Energy*, vol. 9, no. 1, pp. 12–23, Jan. 2018.

[44] H. Tao, H. Hu, X. Wang, F. Blaabjerg, and Z. He, “Impedance-based harmonic instability assessment in a multiple electric trains and traction network interaction system,” *IEEE Trans. Ind. Appl.*, vol. 54, no. 5, pp. 5083–5096, Sep. 2018.

[45] H. Hu, H. Tao, F. Blaabjerg, X. Wang, Z. He, and S. Gao, “Train–network interactions and stability evaluation in high-speed railways—Part I: Phenomena and modeling,” *IEEE Trans. Power Electron.*, vol. 33, no. 6, pp. 4627–4642, Jun. 2018.

[46] H. Hu, H. Tao, X. Wang, F. Blaabjerg, Z. He, and S. Gao, “Train–network interactions and stability evaluation in high-speed railways—Part II: Influential factors and verifications,” *IEEE Trans. Power Electron.*, vol. 33, no. 6, pp. 4643–4659, Jun. 2018.

[47] Y. Zhan, X. Xie, H. Liu, H. Liu, and Y. Li, “Frequency-domain modal analysis of the oscillatory stability of power systems with high-penetration renewables,” *IEEE Trans. Sustain. Energy*, vol. 10, no. 3, pp. 1534–1543, Jul. 2019.

[48] X. Zhu, H. Hu, H. Tao, and Z. He, “Stability analysis of PV plant-tied MVdc railway electrification system,” *IEEE Trans. Transp. Electrific.*, vol. 5, no. 1, pp. 311–323, Mar. 2019.

[49] H. Hu, X. Wang, Y. Peng, Y. Xia, M. Yu, and W. Wei, “Stability analysis and stability enhancement based on virtual harmonic resistance for meshed DC distributed power systems with constant power loads,” *Energies*, vol. 10, no. 1, Jan. 2017, Art. no. 69.

[50] W. Zhou, R. E. Torres-Olguin, M. K. Zadeh, B. Bahrani, Y. Wang, and Z. Chen, “Electromagnetic oscillation origin location in multiple-inverter-based power systems using components impedance frequency responses,” *IEEE Open J. Ind. Electron. Soc.*, vol. 2, pp. 1–20, Jan. 2021.

[51] A. I. Semlyen, “S-domain methodology for assessing the small signal stability of complex systems in nonsinusoidal steady state,” *IEEE Trans. Power Syst.*, vol. 14, no. 1, pp. 132–137, Feb. 1999.

[52] L. Fan and Z. Miao, “Admittance-based stability analysis: Bode plots, Nyquist diagrams or eigenvalue analysis?,” *IEEE Trans. Power Syst.*, vol. 35, no. 4, pp. 3312–3315, Jul. 2020.

[53] Y. Zhan, X. Xie, H. Liu, H. Liu, and Y. Li, “Frequency-domain modal analysis of the oscillatory stability of power systems with high-penetration renewables,” *IEEE Trans. Sustain. Energy*, vol. 10, no. 3, pp. 1534–1543, Jul. 2019.

[54] A. Suarez and F. Ramirez, “Two-level stability analysis of complex circuits,” *IEEE Trans. Microw. Theory Technol.*, vol. 69, no. 1, pp. 132–146, Jan. 2021.

[55] W. Cao, Y. Ma, L. Yang, F. Wang, and L. M. Tolbert, “D–Q impedance based stability analysis and parameter design of three-phase inverter-based AC power systems,” *IEEE Trans. Ind. Electron.*, vol. 64, no. 7, pp. 6017–6028, Jul. 2017.

[56] H. Zhang, X. Wang, M. Mehrabankhomartash, M. G. Saeedifard, Y. Meng, and X. Wang, “Harmonic stability assessment of multi-terminal DC (MTDC) systems based on the hybrid AC/DC admittance model and determinant-based GNC,” *IEEE Trans. Power Electron.*, vol. 37, no. 2, pp. 1653–1665, Feb. 2022.

[57] A. Rygg and M. Molinas, “Apparent impedance analysis: A small-signal method for stability analysis of power electronic-based systems,” *IEEE J. Emerg. Sel. Topics Power Electron.*, vol. 5, no. 4, pp. 1474–1486, Dec. 2017.

[58] R. Hassan, H. Wang, M. M. Ur Rehman, B. Riar, and R. Zane, “Nodal impedance-based stability analysis of DC nanogrids,” in *Proc. IEEE 19th Workshop Control Modelling Power Electron. (COMPEL)*, Padua, Italy, Jun. 2018, pp. 1–7.

[59] A. Riccobono and E. Santi, “Stability analysis of an all-electric ship MVDC power distribution system using a novel passivity-based stability criterion,” in *Proc. IEEE Electr. Ship Technol. Symp.*, Arlington, VA, USA, Apr. 2013, pp. 411–419.

[60] W. Chen, *Introduction to Complex Analysis*, 2002. [Online]. Available: http://williamchen-mathematics.info/lnicafolder/lnica.html

[61] J. Fang, “Research on power sharing and impedance stability analysis of DC power distribution system with multi-converter inserted,” Ph.D. dissertation, Hunan Univ., China, 2021.

[62] D. Lumbreras, E. L. Barrios, A. Urtasun, A. Ursua, L. Marroyo, and P. Sanchis, "On the stability of advanced power electronic converters: The generalized bode criterion," *IEEE Trans. Power Electron.*, vol. 34, no. 9, pp. 9247–9262, Sep. 2019.

[63] J. Samanes *et al.*, "Control design and stability analysis of power converters: The MIMO generalized bode criterion," *IEEE J. Emerg. Sel. Topics Power Electron.*, vol. 8, no. 2, pp. 1880–1893, Jun. 2020.

[64] J. J. Grainger and W. D. Stevenson, *Power System Analysis*. New York, NY, USA: McGraw-Hill, 1994.

[65] B. Zhang, S. Chen, and Z. Yan, *Analysis of Advanced Power Network*, 2nd ed. Beijing, China: Tsinghua Univ. Press, 2007.

Bangbang He (Student Member, IEEE) was born in Henan, China, in 1994. He received the B.S. and M.S. degrees in electrical engineering from the China University of Mining and Technology, Beijing, China, in 2017 and 2020, respectively. He is currently working toward the Ph.D. degree in electrical engineering with Southeast University, Nanjing, China.

His research interests include modeling and stability analysis of power electronics-based power system, and energy saving of railway traction system.

Wu Chen (Senior Member, IEEE) was born in Jiangsu, China, in 1981. He received the B.S., M.S., and Ph.D. degrees in electrical engineering from the Nanjing University of Aeronautics and Astronautics (NUAA), Nanjing, China, in 2003, 2006, and 2009, respectively.

From 2009 to 2010, he was a Senior Research Assistant with the Department of Electronic Engineering, City University of Hong Kong, Hong Kong. In 2010 and 2011, he was a Postdoctoral Researcher with Future Electric Energy Delivery and Management Systems Center, North Carolina State University, Raleigh, NC, USA. Since September 2011, he has been an Associate Research Fellow with the School of Electrical Engineering, Southeast University, Nanjing, China, where he has been a Professor since 2016. His main research interests include soft-switching converters, power delivery, and power electronic system integration.

Dr. Chen is an Associate Editor for for IEEE TRANSACTIONS ON INDUSTRIAL ELECTRONICS, *Journal of Power Electronics*, and *CPSS Transactions on Power Electronics and Applications*.

Xinbo Ruan (Fellow, IEEE) received the B.S. and Ph.D. degrees in electrical engineering from the Nanjing University of Aeronautics and Astronautics (NUAA), Nanjing, China, in 1991 and 1996, respectively.

In 1996, he joined the Faculty of Electrical Engineering Teaching and Research Division, NUAA, where he became a Professor with the College of Automation Engineering in 2002 and has been engaged in teaching and research in the field of power electronics. From August 2007 to October 2007, he was a Research Fellow with the Department of Electronic and Information Engineering, Hong Kong Polytechnic University, Hong Kong, China. From March 2008 to September 2011, he was also with the School of Electrical and Electronic Engineering, Huazhong University of Science and Technology, Wuhan, China. He has authored or coauthored 11 books and more than 300 technical papers in journals and conferences. His main research interests include soft-switching dc–dc converters, soft-switching inverters, power factor correction converters, modeling the converters, power electronics system integration, and renewable energy generation system.

Dr. Ruan has been a member of the Technical Committee on Renewable Energy Systems within the IEEE Industrial Electronics Society since 2008. He is currently an Associate Editor for IEEE TRANSACTIONS ON INDUSTRIAL ELECTRONICS, IEEE TRANSACTIONS ON POWER ELECTRONICS, *IEEE Journal of Emerging and Selected Topics on Power Electronics, IEEE Open Journal of the Industrial Electronics Society*, AND IEEE TRANSACTIONS ON CIRCUITS AND SYSTEMS–II. From 2005 to 2013, and since 2017 again, he has been a Vice President with China Power Supply Society (CPSS). He was a recipient of the Delta Scholarship by the Delta Environment and Education Fund in 2003 and Special Appointed Professor of the Chang Jiang Scholars Program by the Ministry of Education, China, in 2007.

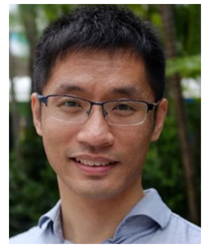

Xin Zhang (Senior Member, IEEE) received the Ph.D. degree in automatic control and systems engineering from the University of Sheffield, Sheffield, U.K., in 2016, and the Ph.D. degree in electronic and electrical engineering from the Nanjing University of Aeronautics and Astronautics, Nanjing, China, in 2014.

From 2017 to 2020, he was an Assistant Professor of power engineering with the School of Electrical and Electronic Engineering, Nanyang Technological University, Singapore. He is currently a Professor with Zhejiang University, Hangzhou, China. His research interests include power electronics, power systems, and advanced control theory, together with their applications in various sectors.

Dr. Zhang is the Associate Editor IEEE TIE/JESTPE/OJPE/ACCESS and IET Power Electronics. He was the recipient of the highly prestigious Chinese National Award for Outstanding Students Abroad, in 2016.

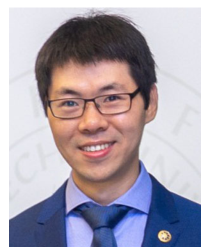

Zhixiang Zou (Senior Member, IEEE) received the B.Eng. and Ph.D. degrees in electrical engineering from Southeast University, Nanjing, China, in 2007 and 2014, respectively, and the Dr.-Ing. degree *(summa cum laude)* from Kiel University, Kiel, Germany, in 2019.

He was an Engineer with State Grid Electric Power Research Institute, Nanjing, China, from 2007 to 2009. He was a Research Fellow and Lecturer with the Chair of Power Electronics, Kiel University, from 2014 to 2019. He is currently an Associate Professor with the School of Electrical Engineering, Southeast University. His research interests include smart transformers, microgrid stability, modeling, and control of power converters.

Dr. Zou is an Associate Editor for the *IEEE Open Journal of Power Electronics*, an Associate Editor for the *IEEE Access*, an Editor for the *International Transactions on Electrical Energy Systems*, and an Editor for the *Mathematical Problem in Engineering*, and a Standing Director of IEEE PES Power System Relaying and Control Satellite Committee.

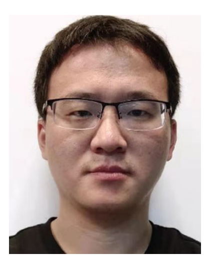

Wu Cao (Member, IEEE) received the B.S., M.S., and Ph.D. degrees in electrical engineering from Southeast University, Nanjing, China, in 2007, 2011, and 2015, respectively.

In 2016, he joined Southeast University, where he is currently an Associate Professor with the School of Electrical Engineering. His research interests include the stability analysis and control of parallel-connected inverters, harmonic current suppression, and reactive power compensation.